HHS Public Access

Author manuscript

Adv Mater. Author manuscript; available in PMC 2024 May 01.

Published in final edited form as:

Adv Mater. 2023 May ; 35(21): e2206370. doi:10.1002/adma.202206370.

Nanoparticle-Mediated Radiotherapy Remodels the Tumor Microenvironment to Enhance Antitumor Efficacy

Wenyao Zhen,

Department of Chemistry, Department of Radiation and Cellular Oncology, and the Ludwig Center for Metastasis Research, The University of Chicago, Chicago, IL 60637, USA

Ralph R. Weichselbaum,

Department of Radiation and Cellular Oncology and the Ludwig Center for Metastasis Research, The University of Chicago, Chicago, IL 60637, USA

Wenbin Lin

Department of Chemistry, Department of Radiation and Cellular Oncology, and the Ludwig Center for Metastasis Research, The University of Chicago, Chicago, IL 60637, USA

Abstract

Radiotherapy (RT) uses ionizing radiation to eradicate localized tumors and, in rare cases, control tumors outside of the irradiated fields via stimulating an antitumor immune response (abscopal effect). However, the therapeutic effect of RT is often limited by inherent physiological barriers of the tumor microenvironment (TME), such as hypoxia, abnormal vasculature, dense extracellular matrix (ECM), and an immunosuppressive TME. Thus, it is critical to develop new RT strategies that can remodel the TME to overcome radio-resistance and immune suppression. In the past decade, high-Z element nanoparticles have been developed to increase radiotherapeutic indices of localized tumors by reducing X-ray doses and side effects to normal tissues and enhance abscopal effects by activating the TME to elicit systemic antitumor immunity. In this review, we will discuss the principles of RT and radiosensitization, the mechanisms of radio-resistance and immune suppression, and the use of various nanoparticles to sensitize RT and remodel TMEs for enhanced antitumor efficacy. We will also highlight the challenges in clinical translation of multi-functional TME-remodeling nanoradiosensitizers.

Graphical Abstract

wenbinlin@uchicago.edu .

The authors declare the following competing financial interest(s): Wenbin Lin is the founder of Coordination Pharmaceuticals, which licensed the nMOF technology from the University of Chicago. Ralph R. Weichselbaum is a consultant to Coordination Pharmaceuticals.

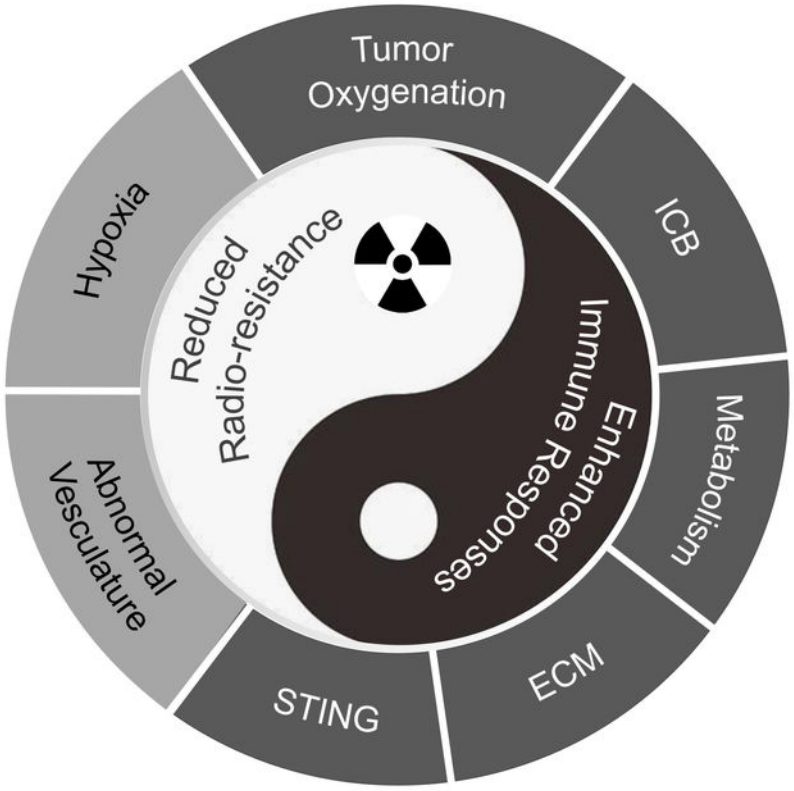

In this review, we discuss the principles of RT and radiosensitization, the mechanisms of radio-resistance and immune suppression, and the use of various nanoparticles to sensitize RT and remodel TMEs for enhanced antitumor efficacy. The challenges in clinical translation of multifunctional TME-remodeling nanoradiosensitizers are also highlighted.

Keywords

Nanoparticle; Cancer; Radiotherapy; Tumor microenvironment remodeling; metal-organic framework

1. Introduction

Despite recent advancements in cancer treatment, more effective therapeutic strategies are needed to treat malignant tumors. By using localized ionizing radiation to cause DNA damage and kill cancer cells, radiotherapy (RT) is used to treat approximately 50% of cancer patients in both curative and palliative settings. Unlike phototherapies, RT utilizes high-energy ionizing radiation to overcome the limitation of tissue penetration and is used to treat both superficial and deep-seated tumors.[1,2] Depending on the radiation source, RT can be categorized as internal and external. In internal RT, therapeutic doses of ionizing radiation are delivered to tumors via intravenous injection or intra-arterial administration of therapeutic radionuclides or by direct implantation of radioisotope-embedded beads into tumors.[3] In external RT, therapeutic doses of ionizing radiation are delivered to tumors using

external beams of photons, electrons, and protons.[4] Both types of RT can directly induce local apoptosis, autophagy, necrosis, or replicative senescence of cancer cells[5] by producing reactive oxygen species (ROS)[6] to cause DNA damage.[7] Advances in hardware and software technologies have provided conformal radiation techniques,[8] which are aided by advanced imaging systems to deliver a desired dose of radiation to the precise location of a tumor, thus maximizing therapeutic effects while minimizing radiation damage to normal organs.[9]

Radiosensitizers can be introduced during RT to enhance the radiotherapeutic effects of ionizing radiation. The radiosensitizers can be classified as 1) chemotherapies such as cisplatin, 5-fluorouracil, and taxanes; 2) gaseous molecules such as O_2, NO, and H_2S; and 3) high-Z elements such as Au, Ba, Bi, Pt, Hf, and W. Chemotherapies presumably enhance RT by arresting cancer cells in the most radiation-sensitive phases of the cell cycle and eliminating radioresistant cells in late S phase but often cause debilitating side effects to cancer patients. Gaseous radiosensitizers enhance RT by increasing ROS production and/or reducing the expression of hypoxia-inducible factor-1α (HIF-1α). It is, however, challenging to ensure therapeutic efficacy due to the difficulty in controlling their concentrations, diffusion rates, and tumor retention. High-Z elements enhance RT by increasing biological reactions and depositing more radiation energy in tumors, via their stronger interactions with secondary photons and electrons, than in normal tissues.[10] In addition to increasing local antitumor effects of RT, the holy grail of radiosensitizer design is to improve the killing of tumor cells outside of the irradiated fields (abscopal effect). An ideal radiosensitizer would enhance RT to produce systemic antitumor effects by inducing immunogenic cell death (ICD), enhancing the presentation of tumor-associated antigens (TAAs), and activating cytotoxic T cells to mount host immune responses.

Although RT is widely used to treat many different types of tumors, it has several limitations. First, radio-resistance is a key impediment to both curative and palliative RT. Previous research on enhancing the effectiveness of RT has mainly focused on cancer cells while neglecting the complicated biological interactions between cancer cells and the tumor microenvironment (TME), which refers to the unique natural environment formed by cancer cells, infiltrating immune cells, tumor-associated fibroblasts (CAFs), blood vessels, lymphatic vessels, secreted factors, and the extracellular matrix (ECM).[11–12] Second, the abscopal effect triggered by RT alone is an infrequent event in the clinic,[13] which likely results from these various elements in the TME. For instance, dense ECM and fibroblasts around solid tumors form a physical barrier for immune cells to enter tumor tissues, whereas exhausted or transiently activated antigen-specific cytotoxic T lymphocytes (CTLs) limit the efficacy of immune checkpoint blockade (ICB) and other immunotherapies. Consequently, it is crucial to understand and modulate the interactions between RT and the TME for maximal therapeutic effects.[14] Third, patients receiving RT and ICB combination treatments may experience more severe side effects than either therapy alone. For example, RT to the chest combined with ICB was associated with a high incidence of pneumonia,[15] whereas abdomen RT combined with ICB increased the incidence of colitis.[16]

Multi-functional nanomaterials with unique thermodynamic, optical, magnetic, electrical and catalytic properties have recently been explored to address the challenges in RT. Many radiosensitizers have been engineered into nanoplatforms to enhance the therapeutic

effect of RT[17, 18] by taking advantage of the enhanced penetration and retention (EPR) effect[19, 20] and the versatility of nanomaterials.[21, 22] The availability of a great number of nanomaterials with high Z-number elements, such as Au,[23] polyoxometalates,[24] and metal oxides (including HfO_2 and WO_{3-x}),[25–27] and nanoscale metal-organic frameworks (nMOFs),[23, 28–31] has paved the way for enhancing radiation energy deposition in tumors. HfO_2 nanoparticle radioenhancer (NBTXR3) was extensively tested in the clinic and received CE marking as a medical device for the treatment of locally advanced soft-tissue sarcoma in 2019.[29, 32] Recently, nanosystems containing both nanoscintillators and photosensitizers have also been developed for X-ray-induced photodynamic therapy (X-PDT) of tumors in animal models.[33–36] In X-PDT, nanosystems first convert X-rays to visible light via photoluminescence by nanoscintillators and then use the visible photons to excite the photosensitizers for PDT[37, 38] Nanoradiosensitizers with the ability to remodel TMEs have been used to reduce radio-resistance by relieving tumor hypoxia or via tumor vascular normalization.[39] Besides enhancing the radiotherapeutic effects on local tumors, nanoradiosensitizers have also been used to boost systemic antitumor immune responses;[40] they remodel the immunosuppressive microenvironment by relieving hypoxia, blocking immune checkpoints, rewiring the metabolic process of cancer cells, and remodeling ECM.[41] Ideal nanoradiosensitizers thus not only sensitize tumors to RT treatment but also modulate the biological processes within the TME to eradicate tumors without causing side effects to normal tissues.[14] It is thus of great fundamental interest and practical significance to develop nanoradiosensitizers to remodel TMEs by exploiting the differences between TMEs and normal tissues.

Herein, we provide a comprehensive overview of recent advances in the design of nanoradiosensitizers for RT enhancement and TME remodeling. We summarize the principles of RT, mechanisms of radio-resistance, and strategies for TME-remodeling radiosensitization by examining several recently studied nanoplatforms. We highlight the latest progress in remodeling TMEs by constructing multi-functional nanoradiosensitizers to ameliorate tumor hypoxia, target abnormal vasculatures, and tumor-associated immune cells, and synergize with ICB (Scheme 1). We also provide our perspectives on enhancing radiosensitization through multi-functionalization of nanomaterials and highlight the challenges in bridging basic discovery of nanoradiosensitizers and their clinical applications. We hope this review will draw research interests from multiple disciplines to discover and translate efficient and safe nanoradiosensitizers for cancer treatment.

2. Remodeling the TME to Overcome Radio-resistance

2.1. Relieving Hypoxic TMEs

Hypoxia is prevalent in many tumor tissues due to the high oxygen consumption by cancer cells, which is further exacerbated by insufficient oxygen delivery via dysfunctional microvasculatures.[42] Hypoxia significantly limits the efficacy of RT by inducing radio-resistance and promoting tumor metastasis.[43, 44] RT can directly or indirectly ionize DNAs to generate DNA free radicals. Oxygen primarily sensitizes RT via oxidation of DNA free radicals to immobilize and enhance DNA damage (Figure 1). Clustered ionization along radiation tracks causes DNA double-strand breaks (DSBs) and oxidizes nucleobases to

damage DNAs. In addition to this classic “oxygen effect”, hypoxia is now known to affect the radio-sensitivity via other mechanisms, including changes in the ROS signaling pathway, inflammation, and DSB repair.[42, 45–46] Consequently, disruption of the diverse processes by which hypoxia influences tumor biology and radio-resistance can restore the antitumor efficacy of RT.

Several approaches have been explored to overcome the limitation of “oxygen effect” during RT,[47] including using hypoxic cytotoxins to destroy hypoxic cancer cells, increasing radiation energy deposition in cancer cells, using small-molecule one-electron oxidants as electron-affinity radiosensitizers to decrease the reliance on O_2, and increasing O_2 concentrations in tumors. In particular, two distinct strategies have been developed to increase O_2 concentrations in tumors: (1) delivering O_2 to tumors through blood transfusion, normobaric oxygen/carbogen breathing, blood substitutes [perfluorocarbon and hemoglobin (Hb)], and hyperbaric oxygen (HBO) and (2) designing nanosystems to catalyze the decomposition of endogenous hydrogen peroxide (H_2O_2) in tumor tissues to O_2.

One strategy to regulate hypoxic TME is through delivering O_2 to tumors using blood substitutes, such as perfluorocarbon and Hb. Dai and coworkers reported the design of oxygen-enriching nanoplatform Hb@Hf-Ce6 (Ce6 is chlorin e6) to relieve hypoxia and improve the therapeutic effect of RT (Figure 2).[48] Hb@Hf-Ce6 was prepared by coordination between Hf (Z=72) and Ce6-modified polyphenols with simultaneous encapsulation of Hb. Hb@Hf-Ce6 enhanced O_2 release over free Hb, and the O_2 release was further enhanced under X-ray irradiation (Figure 2d). It was proposed that X-ray energy absorbed by Hf could activate Ce6 to produce singlet oxygen ($^1O_2$), which in turn kills cancer cells (Figure 2e). This work overcame the limitation of tumor hypoxia and realized RT and radiodynamic therapy (RDT) of cancer, which was first put forward by Lin and coworkers.[6, 49]

Another strategy to overcome hypoxic TME relies on converting high local concentrations of H_2O_2 to generate O_2 through delivering natural enzyme catalase or using nanomaterials with high catalase-like catalytic activities, such as noble metal NPs, metal oxide NPs, Prussian blue NPs, and carbon and nitrogen-based nanomaterials.[51, 52] Liu and coworkers constructed a tantalum oxide (TaO_x)-based PEG-TaO_x@Catalase (PEG is polyethylene glycol) to overcome tumor hypoxia. As shown in Figure 3a, catalase was directly encapsulated into hollow nanospheres of TaO_x by adding tantalum precursor (tantalum ethoxide) into catalase-containing water/ethanol mixture at room temperature. TaO_x@Catalase NPs were further coated with cationic polyallylamine hydrochloride and anionic polyacrylic acid sequentially, and conjugated with amine-terminated PEG (Figure 3a). The resultant PEG-TaO_x@Catalase clearly showed a hollow nanostructure (Figure 3b–3d), which delivered catalase to the tumor and maintained high catalytic activity of catalase. In high H_2O_2 tumor tissues, PEG-TaO_x@Catalase relieved tumor hypoxia by decomposing H_2O_2 and simultaneously induced DNA damage under X-ray irradiation (Figure 3e)[53, 54] without causing obvious toxicity to the treated mice (Figure 3f).[50] The same group also developed core-shell PLGA-R837@catalase NPs consisting of the water-soluble natural catalase core and the poly(lactic-co-glycolic) acid (PLGA) shell loaded with hydrophobic imiquimod (R837), a toll-like-receptor-7 agonist, to relieve tumor hypoxia.[53, 54]

In addition to natural catalase, some nanomaterials with high catalase-like activities are also used to decompose H_2O_2 to O_2 in tumors. For example, Lin and coworkers designed a biomimetic Hf-DBP-Fe nMOF (DBP is 5,15-di(p-benzoato)porphyrin) with porphyrin-$Fe^{III}Cl$ centers to enhance the anticancer effect of RT-RDT in hypoxic tumors (Figure 3g, 3h).[6] They first synthesized Hf-DBP nMOF comprising constructed by Hf_{12} SBUs and DBP ligands through a solvothermal method. Hf-DBP was then treated with $FeCl_2{\cdot}4H_2O$ in ethanol to afford Hf-DBP-Fe with porphyrin-$Fe^{III}Cl$ centers (Figure 3h). Hf-DBP-Fe showed a Hf to Fe ratio of 12 : 7.1, indicating the metalation of all DBP ligands in Hf-DBP with Fe^{III} ions. Hf-DBP-Fe showed a nanoplate morphology of ~100 nm in width (Figure 3i) and 10 nm in thickness (Figure 3j). Hf-DBP-Fe decomposed elevated levels of H_2O_2 to generate O_2 for RT sensitization and hydroxyl radical for chemodynamic therapy (CDT), thus relieving tumor hypoxia and enhancing radiation-triggered DNA damage and the therapeutic efficacy of RT-RDT (Figure 3k).

Hypoxic TMEs with reduced oxygen levels greatly restrict the clinical outcomes of RT.[55] Potential strategies can leverage our increased understanding of the interrelationships between hypoxia and other features of the TME (such as acidosis and cellular interactions) to more effectively overcome hypoxia-induced radio-resistance. As tumors in the same patient may have different levels of hypoxia, noninvasive techniques are needed to accurately and reliably image hypoxia in tumors and to improve clinical outcomes of RT. Hypoxia-sensitive magnetic resonance imaging, positron-emission tomography imaging, computed tomography imaging, photoacoustic imaging, and fluorescence imaging are clearly needed.[56]

2.2. Remodeling Abnormal Tumor Vascular Microenvironment

In many solid tumors, the supply of oxygen and nutrients through normal blood vessels cannot meet the demands for tumor growth. As a result, tumors develop neovasculatures from the normal host vascular network through the process of angiogenesis. These neovasculatures show severe structural and functional abnormalities, such as disorganized vascular structures and their spatial heterogeneity, which leads to insufficent supply of oxygen to the developing tumor.[57] These hypoxic areas in tumors are radio-resistant, leading to poorer clinical outcomes after RT treatment.[58] In addition, aberrant vascular morphology and a decrease in vessel density can also lead to an inadequate perfusion of nanomedicines in tumors. Because the vascular network has been considered a prime target to alleviate tissue damage,[4] the idea of remodeling tumor vasculatures to enhance RT efficiency has attracted significant research interest.[4] The high interstitial pressure generated by the growth of tumor cells and increased secretion of pro-angiogenic factors (e.g., vascular endothelial growth factor (VEGF)) by tumor cells are the primary causes of tumor vascular abnormalities.[59] Currently, the normalization of tumor blood vessels is realized through many strategies, including blockade of angiogenic factor expression with the anti-VEGF agent cediranib and inhibition of angiopoietin-2 (Ang-2) with the antibody MEDI3617. Normalization of tumor blood vasculatures can significantly enhance the accumulation of nanoparticles at the tumor site. Permeabilization of tumor blood vessels and degradation of ECM have similar functions.[60–62]

The efficiency of traditional anti-angiogenic therapies is often limited by drug resistance due to cancer cells' ability to bypass these therapies by activating compensatory pathways to restore angiogenesis in the tumor tissue. Wang and coworkers modified gold (Au) NPs with the reaction product of sodium alginate (SA) and 8-quinoline boric acid (QBA) to afford Au@SA-QBA for simultaneously targeting multiple pathways involved in angiogenesis and overcoming severe hypoxia resulting from abnormal blood vessels in the TME.[63] With high chemical stability and biocompatibility, high-Z Au NPs have been examined as an efficient nanoradiosensitizer to enhance RT.[63] SA-QBA delivered by Au@SA-QBA reacted with H_2O_2 to form 8-hydroxy-quinoline (8-HQ), which is a strong chelator for iron and has antioxidation properties. 8-HQ thus reduces oxidative pressure and the expression of many angiogenic factors, such as angiopoietin-2, VEGF, and fibroblast growth factor. Consequently, treatment with Au@SA-QBA increased the pericyte coverage by 32% and blood perfusion by 78%, which in turn regulated tumor leakage while alleviating tumor hypoxia and induced vascular normalization.[64, 65] Upon 4 Gy X-ray irradiation, Au@SA-QBA enhanced tumor growth inhibition by 38.6% over Au@SA,[8] suggesting the enhancement of RT efficacy via normalization of tumor blood vessels by simultaneously modulating multiple pathways involved in angiogenesis.

In addition to causing hypoxia, distorted blood vessels and relatively undeveloped lymphatic systems also limit penetration of nanomaterials in tumors.[67, 68] Many efforts have been made to address this issue. Liu and coworkers prepared ^{131}I-labeled liposomal NPs to facilitate the uptake of second-wave therapeutic NPs into tumor tissues for enhancing internal radioisotope therapy (RIT) of cancer through normalizing tumor blood vasculature. They radiolabeled liposomes by first encapsulating bovine serum albumin (BSA) in liposomes and then radiolabeled BSA via reacting tyrosine residues of BSA with $^{131}I_2$ to greatly improve radiolabeling stability (Figure 4a). After i.v. injection, the ^{131}I-labeled liposome with a long blood circulation half-life was trapped near blood vessels and emitted β-rays to destroy endothelial cells (Figure 4b, 4c). Subsequently, second-wave liposomal NPs were efficiently retained in the tumor tissue due to the RIT-enhanced EPR effect (Figure 4d). Three parallel experiments were conducted to show that pre-treatment of RIT with ^{131}I-BSA-liposome could enhance the therapeutic outcomes of photothermal therapy, chemotherapy, and ICB therapy.[66]

3. Remodeling the TME to Reinforce Radiation-Induced Immune Responses

Cancer immunotherapies, including chimeric antigen receptor T cell (CAR-T) therapy, cancer vaccines, and ICB, rely on the body's immune system to fight cancer.[69] Immune organs and immune cells play crucial roles in these processes.[70] Immune organs mainly include primary lymphoid organs, such as the bone marrow and thymus, and secondary lymphoid organs, such as the spleen and lymph nodes. Immune cells mainly include lymphocytes (T cells, B cells, and natural killer (NK) cells), myeloid cells (macrophages and dendritic cells (DCs)), and granulocytes. Among them, helper T cells and CTLs can directly recognize and destroy infected or transformed cells, while B lymphocytes produce antibodies to fight offending microorganisms and tumor cells.[71] Antigen-presenting

cells (APCs) represent another important class of immune cells. DCs are the most important and functional APCs due to their large surface area and high expression of major histocompatibility complex (MHC) molecules.[72] In the presence of “danger signals,” immature DCs undergo a “maturation process” of cytoskeletal rearrangement, dendrite formation, and cell surface up-regulation of MHC class I and MHC class II molecules. Mature DCs migrate to regional lymph nodes through lymphatic vessels and present antigens in the form of polypeptides (antigen epitopes) to $CD8^+$ CTLs and/or $CD4^+$ helper T lymphocytes. Under stimulation of mature DCs, antigen-specific T cells can proliferate, become activated in the lymph, and migrate to tumor sites to exert cytotoxicity on cancer cells (Scheme 2).[72]

To protect the host from autoimmunity, many types of immune checkpoints exist as inhibitory regulators of the immune system. For example, T lymphocytes express programmed cell death protein-1 (PD-1), cytotoxic T lymphocyte-associated protein 4 (CTLA4), lymphocyte activating factor-3 (LAG-3), and B- and T-lymphocyte attenuation factor (BTLA) on their surfaces.[73] In addition, programmed cell death-ligand 1 (PD-L1), a transmembrane protein that binds to PD-1, is over-expressed on the surface of tumor cells to facilitate immune escape (Scheme 2). Many immune checkpoint inhibitors (ICIs), including anti-CTLA4, anti-PD-1, and anti-PD-L1 antibodies, have been developed to block immune checkpoints and thus invigorate T cells; several ICIs have been approved by the US Food and Drug Administration (FDA) for cancer immunotherapy.[73]

In 1953, Mole and coworkers first proposed that RT could cause abscopal effect, the responses of tumors outside of the irradiated fields during RT.[74] It is believed that RT has immunomodulatory effects which induce abscopal effect. However, the abscopal effect triggered by RT alone is a rare event in human patients, likely due to limited immune activation by RT. Many therapeutic approaches have been combined with RT with the hope of increasing abscopal effect to elicit potent systemic antitumor efficacy.[13]

Immunosuppressive properties of TMEs prevent effective lymphocyte priming and reduce immune cell infiltration, thus dampening the effects of cancer immunotherapy.[75] For example, hypoxia is frequently associated with increased T cell exhaustion. Additionally, dense ECM around tumor tissues can act as physical barriers to prevent immune cells from entering deeply into tumors and predominant APC subsets in advanced tumors are immunosuppressive or dysfunctional.[69, 76] Thus, remodeling tumor immune microenvironment may significantly increase immune responses triggered by RT.

In recent years, nanoparticles have been developed as potent immune modulators to augment antitumor immune responses of RT by taking advantage of their unique physical and chemical properties.[77–83] First, nanoparticles can accumulate in lymph nodes, spleen and other lymphatic organs to elicit immune responses due to their tunable structures and sizes.[84, 85] Second, nanoparticles can be modified with active targeting molecules for selective delivery of immune-activating drugs to specific immune cells, such as DCs and T cells.[86, 87] Third, nanocarriers can achieve sustained release of multiple drug payloads to simultaneously exert synergistic therapeutic functions.[86–89] In this section, we summarize

recent advances in remodeling tumor immune microenvironments with nanotherapeutics to reinforce the immune response of RT.

3.1. Tumor Oxygenation

Tumor hypoxia is an obstacle to antitumor immunity, with immunohistochemical staining showing an inverse spatial distribution between hypoxia and T cells. T cells often have a perivascular localization in tumor lesions, with greater density around peripheral versus deep tumor vessels.[90] Furthermore, tumors with higher rates of O_2 consumption are often associated with increased T cell exhaustion and reduced antitumor immunity.[91] Consequently, tumor hypoxia is often correlated to lower response rates and shorter survival of patients with recurrent and metastatic tumors.[92–94] Transiently occluded tumor blood vessels can increase tumor hypoxia to cause arrest in T cell motility. In contrast, the elimination of tumor hypoxia can stimulate the function of neutrophils, T cells, and NK cells and also inhibit the activity of regulatory T (Treg) cells.[95–99]

As mentioned in Section 2.1, directly delivering oxygen to tumor tissue or catalyzing the decomposition of H_2O_2 can alleviate immunosuppression caused by hypoxia.[49] Liu and coworkers remodeled hypoxic and immunosuppressive TMEs by inhibiting the expression of HIF-α with a multi-functional ^{32}P-labeled Zn[Fe(CN)$_5$(NO)] nanosheet, which was prepared by mixing zinc ions with the clinical anti-hypertensive drug sodium nitroprusside and then labeled with $Na_2H^{32}PO_4$ (Figure 5a). In addition to directly killing tumor cells, the high-energy particle beam released by ^{32}P also triggered Cerenkov luminescence (CL) (Figure 5b) to stimulate the continuous release of NO from the nanosheets (Figure 5c). The released NO modulated the immunosuppressive TME by inhibiting the expression of HIF-α (Figure 5d), which in turn increased the infiltration of cytotoxic T cells and decreased the levels of immunosuppressive cell types such as Treg cells and tumor-associated macrophages in the tumor tissue (Figure 5e–5i). Local RT of ZnFe(CN)$_5$NO(P^{32}) nanosheets realized potent immune responses, long-term immune memory effects, and effective inhibition of distant tumors.[100]

3.2. Immune Checkpoint Blockade

ICB is a therapeutic strategy that restores exhausted T cells by targeting immune checkpoint molecules such as PD-1 and CTLA-4 to revive antitumor immunity.[102] ICIs have realized remarkable antitumor immune responses in immunogenic tumors through blocking immune checkpoint molecules and their ligands.[103] There are several major classes of ICIs, including those targeting PD-1, such as nivolumab and pembrolizumab, and those targeting PD-L1, such as durvalumab and atezolizumab, and those targeting CTLA-4, such as ipilimumab or tremelimumab. The inhibition of PD-1 or PD-L1 primarily reverses T cell exhaustion, while anti-CTLA-4 inhibit the immunosuppressive activity of Treg cells and increase the ratio of $CD8^+$ T cells to Treg cells in the TME. A number of ICIs, including anti-CTLA-4 monoclonal antibody ipilimumab and PD-1 monoclonal antibodies nivolumab and pembrolizumab, have been approved by the FDA for the treatment of melanoma, non-small cell lung cancer, head and neck cancer, and other tumors.[104–106] Preclinical and clinical evidence indicates that ICIs can be combined with RT to improve the therapeutic outcomes.

Many nanoradiosensitizers composed of high-Z number elements or loaded with immune adjuvants have been developed and combined with anti-PD1/PD-L1 to enhance their therapeutic efficacy. For example, Lin and coworkers designed two porous Hf-based nMOFs, Hf_6-DBA (DBA: 2,5-di(p-benzoato)aniline) and Hf_{12}-DBA nMOFs, as radioenhancers for RT with low-dose X-rays (Figure 6a).[101] These nMOFs not only facilitate the diffusion of short-lived ROS because of their porous structures, but also enhance the energy deposition of RT by trapping secondary photons and electrons within the periodic structures of nMOFs. Compared with Hf_6-DBA, which has a spherical morphology, Hf_{12}-DBA with its plate-like shape showed an enhanced generation of ROS (Figure 6b), which results from more effective X-ray absorption of Hf_{12} clusters over Hf_6 clusters and more facile ROS diffusion due to the thin nanoplate structures (Figure 6c, 6d). Combination of nMOF-mediated RT with anti-PD-L1 elicited a strong abscopal effect to regress both primary (Figure 6e) and distant tumors (Figure 6f). This work showed the potential of combining nMOF-mediated RT with ICB to enhance systemic antitumor immunity in non-T cell-inflamed tumors.[101]

Liu and coworkers developed a novel hydrogel that released immune adjuvants in response to repeated radiation (Figure 7a). Adenosine triphosphate (ATP)-specific aptamer hybridized with immunoadjuvant CpG oligonucleotide was conjugated with alginate (ALG), which formed a hydrogel in situ after intra-tumoral injection (Figure 7b). Interestingly, low doses of oxaliplatin (OxPt) or X-rays triggered the release of ATP for competitive binding with ATP-specific aptamer to trigger the release of CpG while simultaneously inducing ICD of cancer cells. The hydrogel could thus release the immune adjuvant upon X-ray radiation to achieve synergistic responses in regressing primary and re-challenged / metastatic tumors via immune memory, especially when in combination with anti-PD-1 (Figure 7c, 7d).[107] This study provided a strategy for boosting cancer immunotherapy with clinically relevant fractionated chemo- or radio-therapy.[108–111]

Victor et al. reported that the combination of RT and anti-CTLA-4 was more effective than either treatment alone by using the highly immunogenic B16-F10 melanoma mouse model.[111] In a phase I clinical trial of 22 patients with advanced melanoma,[111] a single lesion was exposed to hypofractionated stereotactic body radiation (6~8 Gy/fraction for two or three fractions), followed by four cycles of the CTLA-4 antibody ipilimumab after the last fraction of RT. Although some partial responses (18%) were observed, the majority of the patients (64%) had progressive disease. Other trials tested RT and anti-CTLA-4 combination treatments on unresectable pancreatic cancer (NCT02311361), metastatic NSCLC (NCT02221739), metastatic castration-resistant prostate tumor (NCT00861614), advanced cervical tumor (NCT01711515), and metastatic liver and lung cancers (NCT02239900). A key objective of these combination trials was to identify predictive or prognostic biomarkers.[110]

Although ICB has achieved durable responses in a small subset of cancer patients, the majority of cancer patients do not respond to ICB due to low immunogenicity and inadequate T cell infiltration in their tumors.[101, 107, 108] Systemic injection of immunomodulators carries the risk of adverse immune responses. For example, although CD47 is a checkpoint of the innate immune system,[109–110] it is also widely expressed in

the cells of many non-malignant tissues.[109–111] Off-target inhibition of CD47 can have detrimental effects and, in severe cases, may even lead to cytokine release syndrome (CRS), which can be fatal. New methods are needed to selectively and precisely deliver immunomodulators to the TME to overcome radio-resistance or immunosuppression.[5]

3.3. Metabolic Regulation

To meet the nutrient needs of fast proliferation, cancer cells undergo less efficient aerobic glycolysis to quickly generate ATP and other metabolic intermediates.[112, 113] During this process, lactic acid, a byproduct of aerobic glycolysis, gradually accumulates in tumors to acidify the TME.[114. 115] The altered metabolism of cancer cells not only is conducive to their survival, proliferation, and metastatic spread, but also promotes immunosuppression through enhancing the exhaustion and apoptosis of CTLs and the infiltration of immunosuppressive immune cells to the TME.[116, 117] In addition, ectoenzymes related to nutrient depletion, such as indoleamine 2,3-dioxygenase 1 (IDO-1), CD73, and arginase 1, are overexpressed in the TME to adapt to the fast rate of tumor growth, which enables solid tumors to escape from immune surveillance by causing exhaustion and apoptosis of T cells and NK cells while stimulating immunosuppressive cells including Tregs, tumor-associated macrophages, and myeloid-derived suppressor cells (MDSCs).[115, 108–121] Novel nanoradiosensitizers are needed to overcome the immunosuppression and acid TMEs caused by the altered metabolism of cancer cells.

Recent discoveries have shown that metabolic regulators can reprogram immunosuppressive metabolic TMEs to enhance the therapeutic effects of many cancer treatments.[122] For example, IDO-1 inhibitors were shown to enhance the therapeutic effect of RT through remodeling immunosuppressive TMEs induced by the accumulation of kynurenine (Kyn).[49] Lin and coworkers designed IDO inhibitor (IDOi)-loaded nMOFs to realize low-dose X-ray radiotherapy and strong abscopal responses in murine tumor models (Figure 8a).[49] The DBP-Hf nanoplates (Figure 8b) were composed of $Hf_{12}(\mu_3\text{-}O)_8(\mu_3\text{-}OH)_8(\mu_2\text{-}OH)_6(RCO_2)_{18}$ SBUs and DBP bridging ligands (Figure 8c). It was proposed that the SBUs of Hf could not only absorb X-ray photons for producing •OH via RT but also transfer energy to photosensitizing DBP ligands for $^1O_2$ generation to enable an RDT process (Figure 8a). The combination of PS and Hf-based SBUs simultaneously realized RT and RDT with low-dose X-rays. Intra-tumoral injection of DBP-Hf generated •OH and $^1O_2$ through RT-RDT process, leading to effective ICD (Figure 8d) and, as a result, significantly increased percentages of helper $CD4^+$ T cells (Figure 8e) and cytotoxic $CD8^+$ T cells (Figure 8f) in both primary and distant tumors. The tumors in the DBP-Hf plus intravenous IDOi group were obviously larger than those in the IDOi@DBP-Hf group at day 9 post-treatment. The tumors treated with IDOi@nMOFs without X-ray irradiation showed no obvious inhibition of tumor growth, demonstrating that only the combination of IDOi and nMOF-enabled RT-RDT achieved the abscopal effect to regress local tumors (Figure 8g) and inhibit distant tumors (Figure 8h). This nMOF-mediated RT-RDT together with IDO inhibition could not only treat deep-seated local tumors but also elicit efficient therapeutic effects on distant tumors via systemic antitumor immunity without causing side effects on normal organs.

Liu and coworkers also designed a pH-responsive nanoplatform to enhance the therapeutic effect of RT by decorating calcium carbonate ($CaCO_3$) NPs with a 4-phenylimidazole (4PI)-Zn coordination organic polymer (COP) shell (Figure 9b–9e). 4PI is an inhibitor against IDO-1 (Figure 9a). $CaCO_3$ was prepared via gas diffusion method (Figure 9b) and it can reduce tumor acidity by reacting with protons in the TME, thereby enhancing the therapeutic efficiency of immunotherapy.[123–125] This pH-responsive nanoplatform, denoted as acidity-IDO1 modulation NPs (AIM), could neutralize protons (Figure 9f) and release water-insoluble 4PI to inhibit IDO1-mediated production of Kyn.[126] AIM NPs enhanced RT efficacy against tumors through reversing acidity-triggered radio-resistance and inhibiting the generation of immunosuppressive Kyn (Figure 9g). It was observed that the tumor-infiltrating CTLs, pro-inflammatory M1-type macrophages, and NK cells increased in tumors while the number of immunosuppressive MDSCs, Tregs, and M2-type macrophages decreased. The combination therapy of AIM NPs and X-ray irradiation completely suppressed the growth of CT26 tumors (Figure 9h), effectively inhibited the growth of untreated distant tumors (Figure 9i) via the abscopal effect, and prevented tumor recurrence via the immune memory effect. This work demonstrated the impact of simultaneous neutralization of acidic TMEs and IDO1 inhibition on increasing RT efficacy and preventing tumor metastasis and recurrence.[126, 127] The same research group also prepared a fluorinated calcium carbonate ($fCaCO_3$) nanoregulator by coating $CaCO_3$ NPs with dopamine-grafted perfluorosebacic acid (DA_2-PFSEA) and ferric ions.[128] They found that the as-prepared PFCE@$fCaCO_3$-PEG could reverse the immunosuppressive TME by neutralizing the acidic TME, which was demonstrated by effective inhibition of unirradiated or rechallenged tumors.

The upregulated glycolysis in cancer cells is accompanied by elevation of HIF-1α and its target pyruvate dehydrogenase kinase 1 (PDK1), which restricts the process of pyruvate entering the citric acid cycle, resulting in reduced consumption of mitochondrial oxygen. PDK1 inhibition could regulate the glucose metabolism and enhance oxygen consumption of cancer cells, thus re-sensitizing tumor cells to RT. PDK inhibitors, such as dichloroacetate, could activate the activity of mitochondria and force glycolytic tumor cells into oxidative phosphorylation to reverse RT-induced glycolytic shift.[129] Other drugs that target the enzymes and transporters involved in glucose metabolism, including hexokinase (HK), glucose transporter 1 (GLUT1), and lactate dehydrogenase A (LDHA), have also been used to inhibit glycolysis.[130–134] These inhibitors hold great promise in enhancing RT and for clinical translation to treat patients with advanced tumors.

3.4. Modulation of the Extracellular Matrix

ECM, CAFs, and other factors in the TMEs can also be modulated to remodel the TME and enhance the immune response of RT. However, few studies have been performed to understand how these factors influence the immunosuppressive TEM and impact the efficacy of RT. We will briefly discuss how ECM and CAF mediate immunosuppressive TMEs, and we hope this discussion will inspire the design of nanoradiosensitizers to modulate ECM and CAF to enhance the efficacy of RT.

ECM is mainly composed of proteins secreted by cells, such as collagen, proteoglycan, fibronectin, elastin, and integrin, located in the stroma of the basement membrane and interstitial space as a structural and biochemical support for neighboring cells. ECM acts as a dense physical barrier to the infiltration of peripheral T cells and nanotherapeutics. Among the components of the ECM, collagen is a diverse protein family with at least 28 categories of proteins. In addition to providing structural support, collagen also regulates signaling pathways such as transforming growth factor-β (TGF-β)/Smad, mitogen-activated protein kinase (MAPK), Wnt, and nuclear factor kappa B (NF-κB). Hyaluronic acid (HA) is another essential component of tumor ECM and is over-expressed in ~30% of tumors. Both collagen and HA are potential targets for tumor intervention.

Radiation has been shown to influence ECM interactions, cell adhesion, and intercellular communication by integrin receptors.[135] Recent efforts have been devoted to targeting ECM or eliminating ECM structure to enhance nanomaterial-mediated RT through regulating the immunosuppressive TME and promoting peripheral T cell infiltration.[136] For example, Shi and coworkers reported a ^{131}I-labeled multi-functional dendrimer linked with chlorotoxin (CTX) to target matrix metalloproteinase-2 (MMP2) overexpressed in glioma cancer cells.[137] The ^{131}I-labeled multi-functional dendrimer showed good biocompatibility and enhanced the efficacy of RT. Rationally designed nanoparticles can synergize with degrading enzymes, such as hyaluronidase (HAase),[138] matrix metalloproteinases, and other proteases to decompose intact collagen and its catabolic proteins as well as to eliminate ECM. We believe that multi-functional nanoradiosensitizers have the potential to combine with these natural enzymes to remodel immunosuppressive TMEs for enhanced RT efficacy.

CAFs are stromal cells with a fibroblast-like morphology in tumors. CAFs are phenotypically and epigenetically distinct from normal fibroblasts and are involved in all phases of tumor development.[139–141] Together with other ECM components, CAFs form a strong barrier against the infiltration of nanotherapeutics and immune cells into tumors. CAFs thus play an important role in the therapeutic response to RT by modulating ECM and secreting cytokines or growth factors that could regulate proliferation, invasion, and metastasis of tumors. For instance, CAFs can secrete TGF-β and enhance tumor growth by inhibiting the cytotoxicity of effector T cells. CAFs can also recruit MDSCs and Tregs by upregulating the expression of chemokines, such as chemokine ligand 22 (CCL22) and chemokine ligand 28 (CCL28), to create an immunosuppressive TME. CAFs have also been shown to directly act on T lymphocytes by expressing PD-L1 and PD-L2, inducing exhaustion of T cells and developing immune tolerance. CAFs also secrete exosomes that interact with tumor cells via retinoic acid inducible gene-I (RIG-I) to further increase radio-resistance.

As activated CAFs are strongly associated with immunosuppressive TMEs, targeting activated CAFs and/or directly inhibiting activated fibroblasts in tumor tissues may enhance the efficacy of RT. Lin and coworkers designed a bismuth (Bi)-based nMOF that could modulate the intratumoral biomechanical properties to enhance RT-RDT mediated immune response (Figure 10a).[142] Composed of $Bi_{10}O_8$ cluster SBUs and photosensitizing DBP linkers (Figure 10b–10e), Bi-DBP nMOFs were synthesized via a solvothermal reaction between $Bi(NO_3)_3$ and H_2DBP in a mixed solvent of N,N-dimethylmethanamide

(DMF) and ethanol with trifluoroacetic acid (TFA) as modulator. Bi-DBP showed a nanorod morphology of ~20 nm diameter and ~180 nm length (Figure 10f). Compared to the previously reported Hf-DBP, $Bi_{10}O_8$ clusters bolstered energy deposition and radiosensitization due to their higher absorption cross-section. In addition, the K-edge energy of Bi at 90 keV is higher than that of Hf at 65 keV, which makes Bi more suitable for radiosensitization with clinically used megavolt X-rays. As a result, Bi-DBP generated more ·OH than Hf-DBP under the radiation of X-ray or ^{60}Co-γ-ray. Interestingly, the authors found that Bi-DBP mediated RT/RDT repolarized immunosuppressive M2 macrophages to the M1 phenotype (Figure 10g), lowered tumoral elasticity but increased viscosity (Figure 10h), decreased the stiffness of tumors (Figure 10i), reduced the concentration of TGF-β (Figure 10j), collagen density and inactivated CAFs with down-regulated expression of α-smooth muscle actin (α-SMA). These results showed that Bi-DBP mediated RT/RDT could soften the tumor tissue and modulate tumor biomechanics to facilitate the infiltration of T cells into tumor tissues. Combination therapy with ICB reversed the immuno-suppressive TME to enhance the therapeutic outcomes. This work shows that optimal nanoradiosensitizers can turn immunologic “cold” tumors “hot” through repolarization of M2 macrophages and modulation of biomechanical properties of the tumor to facilitate the infiltration of immune cells into the TME.

3.5. STING Activation

The stimulator of interferon genes (STING) pathway regulates innate immune responses by converting pathogen-derived DNA and self-DNA in the cytosol to produce 2’,3’-cyclic guanosine monophosphate–adenosine monophosphate (cGAMP). cGAMP activates STING to induce type I interferons (IFN-I) and other inflammatory cytokines through activation of both TANK-binding kinase 1 (TBK1)/interferon regulatory factor 3 (IRF3) and IκB kinase (IKK)/NF-κB signaling pathways.[143] Through generation of cytokines, STING agonists, such as cyclic dinucleotides (CDNs) including c-diGMP, c-diAMP, and cGAMP, activate the maturation of DCs and cross-presentation of tumor antigens for antitumor immunity, leading to excellent antitumor efficacy in preclinical models.[144, 145] Several CDN STING agonists, such as ADU-S100 (NCT03172936) and MK-1454 (NCT03010176) have entered clinical trials.[146] When exposed to high-dose X-rays, damaged DNAs escape from the nuclei of cancer cells and enter into the cytosols to generate cGAMP and activate STING.[147, 148] Thus, it is expected that RT and STING activation may have synergistic antitumor effects.

As systemic STING activation has shown significant toxicity, most STING agonists are intratumorally injected to reduce toxicity and overcome poor bioavailability.[149, 150] Many nanoparticle delivery systems have been developed to enhance cytosolic delivery of STING agonists and increase their biological potency.[151] For example, Zhong and coworkers prepared a reduction-responsive biodegradable chimeric polymersomes (CPs) to enhance tumor retention and cytosolic delivery of ADU-S100,[152] leading to STING activation in the TMEs and tumor draining lymph nodes for tumor regression and survival improvement of B16F10 melanoma-bearing mice over free CDN control.

Lin and coworkers designed a 2D nanoplatform, cGAMP loaded on a nanoscale metal–organic layer (MOL), Hf_{12}-Ir, for simultaneous STING activation and radiosensitization

(Figure 11a–11c).[83] Hf_{12}-Ir MOL was prepared by a solvothermal reaction between $HfCl_4$ and $Ir(DBB)[dF(CF_3)ppy]_2^+$ ligands with trifluoro acidic acid modulators (Figure 11a). Hf_{12}-Ir is composed of periodically arranged Hf_{12} SBUs and DBB-Ir photosensitizer ligands (Figure 11b). Hf_{12}-Ir not only maximally expanded the surface area to achieve potent radiosensitization via a RT-RDT process, but also provided anchoring sites to conjugate cGAMP (Figure 11c). Controlled release of cGAMP realized sustained STING activation of APCs (macrophages and DCs) and secretion of type I IFN and inflammatory cytokines, leading to effective regression of local tumors with 4 out of 6 CT26 tumor-bearing mice completely cured (Figure 11d–11f). The development of novel nanoplatforms for simultaneous radiosensitization and delivery of STING agonists to tumors holds great potential for clinical translation to significantly enhance the therapeutic effects of RT.

4. Conclusions and Perspectives

With deeply penetrating X-rays, external RT has been widely used to treat tumors by generating ROS and causing DNA damage. Although rare, RT has also been shown to kill tumor cells outside of the irradiated fields, likely through stimulating the antitumor immune response by the abscopal effect. However, the therapeutic efficacy of RT is compromised by intrinsic physiological properties of the TME as well as intrinsic tumor cell resistance. This review provides an overview of recent progress on using multi-functional nanoparticles to remodel radioresistant and immuno-suppressive TMEs to enhance antitumor efficacy of RT. A number of interesting nanoplatforms have been developed to overcome radio-resistance by relieving hypoxia and remodeling abnormal tumor vasculature, as well as to reduce immunosuppression by relieving hypoxia, combining with ICB, and regulating metabolic processes, ECM, and fibroblasts. Nevertheless, significant challenges still remain for the clinical translation of these nanoplatforms for enhancing RT efficacy in cancer patients.

First, the radiosensitizing effects of most nanoradiosensitizers remain inadequate for less radio-responsive tumors, such as pancreatic cancer and glioblastoma. More in-depth characterization of nanoradiosensitizers can shed light on the choices of metals, morphologies, and porous structures to significantly enhance the radiosensitizing effects of next-generation nanoradiosensitizers.

Second, the radiosensitizing effects of most nanoradiosensitizers have not been benchmarked against known standards. Unlike phototherapies where delivered doses can be precisely determined, accurate dosimetry of radiation doses presents a significant challenge for most nanomedicine labs. The lack of benchmarking and validation of radiosensitizing effects presents a significant hurdle for potential clinical translation of nanoradiosensitizers.

Third, the understanding of the interactions between nanoradiosensitizers and the complex TME remains primitive and incomplete. As tumor tissue is a highly complex and heterogeneous microenvironment, characterized by hypoxia, abnormal vasculature, mild acidity, thick ECM, over-expression of immunosuppressive proteins, and aberrant metabolic regulation, a deeper understanding of how nanoradiosensitizers behave in the complex TME can provide potential strategies to enhance their radiosensitization efficiency.

Fourth, the potential of theragnostic platforms has not been realized for nanoradiosensitizers. The improvements of technology and instrumentation have greatly benefited the field of radiation oncology, but real-time imaging-guided precision RT and visualization and quantification of potential biomarkers that may predict treatment responses have not been adopted to the study of nanoradiosensitizers. The design of theragnostic nanoradiosensitizers can reveal important insights into anticancer mechanisms and potentially speed up the discovery of potent nanoradiosensitizers for clinical investigation.

Fifth, the complexity of most nanoplatforms for radiosensitization presents the most significant hurdle for clinical translation. The synthetic reproducibility, comprehensive characterization and quality control, and biocompatibility of nanoplatforms are important factors for clinical applications. Clinical experience with NTBXR3, a HfO_2-based nanoradiosensitizer, and RiMO-301, an nMOF-based nanoradiosensitizer, should provide useful roadmaps for the translation of other nanoradiosensitizers into the clinic.

Last but not least, the pharmacokinetics and pharmacodynamics of most nanoradiosensitizers remain uncharacterized. These properties are particularly important for the design of systemically injected nanoradiosensitizers.

Despite these challenges, we remain optimistic about the role of immunostimulatory nanoradiosensitizers in enhancing the therapeutic efficacy of RT in cancer patients. Designing innovative nanoparticles with new modes of action for radiosensitization and TME remodeling remains a promising area of nanomedicine research. The potential benefits of these nanoradiosensitizers to cancer patients have motivated us to launch our research program and should inspire the nanomedicine community to pursue this highly interdisciplinary research direction.

Acknowledgments

We thank Mr. Taokun Luo for proofreading the manuscript. This work was supported by the National Cancer Institute (U01-CA198989 and 1R01CA253655), the University of Chicago Medicine Comprehensive Cancer Center (NIH CCSG: P30 CA014599), and the Ludwig Institute for Metastasis Research for funding support.

Biographies

Wenyao Zhen is a postdoctoral fellow under the joint supervision of Prof. Wenbin Lin and Prof. Ralph R. Weichselbaum at the University of Chicago. She obtained her Ph.D. degree from the University of Science and Technology of China (USTC) in December 2021. Her current research mainly focuses on the design of stimuli-responsive, multi-functional nanoscale MOFs for tumor immune microenvironment activation and combination cancer therapy.

Ralph R. Weichselbaum is the Daniel K. Ludwig Distinguished Service Professor of Radiation and Cellular Oncology Chair, Department of Radiation and Cellular Oncology. His research mainly focused on radiation oncology and cancer immunotherapy. Group website: https://www.uchicagomedicine.org/find-a-physician/physician/ralph-r-weichselbaum.

Wenbin Lin is the James Franck Professor of Chemistry, Radiation and Cellular Oncology, and Comprehensive Cancer Center at the University of Chicago. His research mainly focuses on designing novel supramolecular systems and molecular nanotechnologies for applications in chemical and life sciences. Over the past two decades, his group has pioneered the studies of metal–organic frameworks in many applications, including cancer therapy, bioimaging, earth-abundant metal catalysis, artificial photosynthesis, asymmetric catalysis, and second-order nonlinear optics. He is also the founder of two biopharmaceutical companies, RiMO Therapeutics and Coordination Pharmaceuticals, that are translating his group's discoveries to the clinic. Group website: http://linlab.uchicago.edu/.

References

1. Liang H; Deng L; Hou Y; Meng X; Huang X; Rao E; Zheng W; Mauceri H; Mack M; Xu M, Nat. Commun. 2017, 8, 1. [PubMed: 28232747]
2. Weichselbaum RR; Liang H; Deng L; Fu YX, Nat. Rev. Clin. Oncol. 2017, 14, 3659.
3. Finlay IG; Mason MD; Shelley M, Lancet Oncol. 2005, 6, 392. [PubMed: 15925817]
4. Guipaud O; Jaillet C; Clément Colmou K; François A; Supiot S; Milliat F, Br. J. Radiol. 2018, 91, 20170762. [PubMed: 29630386]
5. Darragh LB; Oweida AJ; Karam SD, Front. Immunol. 2019, 9, 3154. [PubMed: 30766539]
6. Ni K; Lan G; Song Y; Hao Z; Lin W, Chem. Sci. 2020, 11, 7641. [PubMed: 34094142]
7. Mi Y; Shao Z; Vang J; Kaidar-Person O; Wang AZ, Cancer Nanotechnol. 2016, 7, 1. [PubMed: 26900409]
8. Wang Z; Tang Y; Tan Y; Wei Q; Yu W, Cell Commun. Signal 2019, 17, 47. [PubMed: 31101063]
9. Baumann M; Krause M; Overgaard J; Debus J; Bentzen SM; Daartz J; Richter C; Zips D; Bortfeld T, Nat. Rev. Cancer 2016, 16, 234. [PubMed: 27009394]
10. Choi J; Kim G; Cho SB; Im H Jun., J. Nanobiotechnol. 2020, 18, 122.
11. De Palma M; Biziato D; Petrova TV, Nat. Rev. Cancer 2017, 17, 457. [PubMed: 28706266]
12. Koelwyn GJ; Quail DF; Zhang X; White RM; Jones LW, Nat. Rev. Cancer 2017, 17, 620. [PubMed: 28943640]

13. Turchan WT; Pitroda SP; Weichselbaum RR, Clin. Cancer Res. 2021, 27, 5188. [PubMed: 34140404]
14. Barker HE; Paget JT; Khan AA; Harrington KJ, Nat. Rev. Cancer 2015, 15, 409. [PubMed: 26105538]
15. Xiao Z; Wang C; Zhou MH; Li N;Liu S; He Y; Wang Y; Feng J; Yao X; Chen L; Ma B; Yu S; Zeng X; Li C, Ding J, Int. Immunopharmacol. 2018, 61, 363. [PubMed: 29945024]
16. Slovin S; Higano C; Hamid O; Tejwani S; Harzstark A; Alumkal J; Scher H; Chin K; Gagnier P; McHenry M; Beer T, Ann. Oncol. 2013, 24, 1813 [PubMed: 23535954]
17. Lu K; He C; Guo N; Chan C; Ni K; Lan G; Tang H; Pelizzari C; Fu YX; Spiotto MT; Weichselbaum RR; Lin W, Nat. Biomed. Eng. 2018, 2, 600. [PubMed: 31015630]
18. Zhu Z; Wu M; Sun J; Huangfu Z; Yin L; Yong W; Sun J; Wang G; Meng F; Zhong Z, Drug Deliv J. 2021, 28, 2301.
19. Cheng Y; Zhao L; Li Y; Xu T, Chem. Soc. Rev. 2011, 40, 2673. [PubMed: 21286593]
20. Matsumoto Y; Nichols JW; Toh K; Nomoto T; Cabral H; Miura Y; Christie RJ; Yamada N; Ogura T; Kano MR; Matsumura Y; Nishiyama N; Yamasoba T; Bae YH; Kataoka K, Nat. Nanotechnol. 2016, 11, 5338.
21. Wen AM; Steinmetz NF, Chem. Soc. Rev. 2016, 45, 4074. [PubMed: 27152673]
22. Kunjachan S; Ehling J; Storm G; Kiessling F; Lammers T, Chem. Rev. 2015, 115, 10907. [PubMed: 26166537]
23. Nosrati H; Seidi F; Hosseinmirzaei A; Mousazadeh N; Mohammadi A; Ghaffarlou M; Danafar H; Conde J; Sharafi A, Adv. Healthc. Mater. 2022, 11, 2102321.
24. Yong Y; Zhang C; Gu Z; Du J; Guo Z; Dong X; Xie J; Zhang G; Liu X; Zhao Y, ACS Nano 2017, 11, 7164. [PubMed: 28640996]
25. Li Y; Qi Y; Zhang H; Xia Z; Xie T; Li W; Zhong D; Zhu H; Zhou M, Biomaterials 2020, 226, 119538. [PubMed: 31639541]
26. Song G; Cheng L; Chao Y; Yang K; Liu Z, Adv. Mater. 2017, 29, 1700996.
27. Hauser AK; Mitov MI; Daley EF; McGarry RC; Anderson KW; Hilt JZ, Biomaterials 2016, 105, 127. [PubMed: 27521615]
28. Lan G; Ni K; Veroneau SS; Luo T; You E; Lin W, J. Am. Chem. Soc. 2019, 141, 6859. [PubMed: 30998341]
29. Xu Z; Ni K; Mao J; Luo T; Lin W, Adv. Mater. 2021, 33, 2104249.
30. Ni K; Lan G; Chan C; Duan X; Guo N; Veroneau SS; Weichselbaum RR; Lin W, Matter 2019, 1, 1331. [PubMed: 32832885]
31. Xu Z; Luo T; Mao J; McCleary C; Yuan E; Lin W, Angew. Chem. Int. Ed. 2022, 61, e202208685.
32. Bonvalot S; Rutkowski PL; Thariat J; Carrère S; Ducassou A; Sunyach MP; Agoston P; Hong A; Mervoyer A; Rastrelli M, Lancet Oncol. 2019, 20, 1148. [PubMed: 31296491]
33. Sun W; Shi T; Luo; Chen X; Lv P; Lv Y.; Zhuang Y; Zhu J; Liu G.; Chen X.; Chen H, Adv. Mater. 2019, 31, 1808024.
34. Chen W; Zhang JJ, Nanosci. Nanotechnol. 2006, 6, 1159.
35. Wang M; Song J; Zhou F; Hoover A; Murray C; Zhou B; Wang L; Qu J; Chen W, Adv. Sci. 2019, 6, 1802157..
36. Chen H; Sun X; Wang G; Nagata K; Hao Z; Wang A; Li Z; Xie J; Shen B, Mater. Horiz. 2017, 4, 1092. [PubMed: 31528350]
37. Chen H; Wang G; Chuang Y; Zhen Z; Chen X; Biddinger P; Hao Z; Liu F; Shen B; Pan Z; Xie J, Nano Lett. 2015, 15, 2249. [PubMed: 25756781]
38. Zhang C; Zhao K; Bu W; Ni D; Liu Y; Feng J; Shi J, Angew. Chem. Int. Ed. 2015, 54, 1770.
39. Song X; Xu J; Liang C; Chao Y; Jin Q; Wang C; Chen M; Liu Z, Nano Lett. 2018, 18, 6360. [PubMed: 30247918]
40. Korbelik M; Hode T; Lam S; Chen W, Cells 2021 10, 492. [PubMed: 33668932]
41. Yang F; Shi K; Hao Y; Jia Y; Liu Q; Chen Y; Pan M; Yuan L; Yu Y; Qian Z, Bioact. Mater. 2021, 6, 3036. [PubMed: 33778186]
42. Singleton DC; Macann A; Wilson WR, Nat. Rev. Clin. Oncol. 2021, 18, 751. [PubMed: 34326502]

43. Nordsmark M; Bentzen SM; Rudat V; Brizel D; Lartigau E; Stadler P; Becker A; Adam M; Molls M; Dunst J, Radiother. Oncol. 2005, 77, 18. [PubMed: 16098619]
44. Zschaeck S; Löck S; Hofheinz F; Zips D; Mortensen LS; Zöphel K; Troost EG; Boeke S; Saksø M; Mönnich D, Radiother. Oncol. 2020, 149, 189. [PubMed: 32417350]
45. Brown JM, Int. J. Radiat. Oncol. Biol. Phys. 2020, 108, 734. [PubMed: 32473180]
46. Shrieve DC; Harris JW, Chem. Med. 1985, 48, 127.
47. Dewhirst MW; Cao Y; Moeller B; Nat. Rev. Cancer 2008, 8, 425. [PubMed: 18500244]
48. Sang W; Xie L; Wang G; Li J; Zhang Z; Li B; Guo S; Deng CX; Dai Y, Adv. Sci. 2021, 8, 2003338.
49. Lu K; He C; Guo N; Chan C; Ni K; Lan G; Tang H; Pelizzari C; Fu Y-X; Spiotto MT, Nat. Biomed. Eng. 2018, 2, 600. [PubMed: 31015630]
50. Song G; Chen Y; Liang C; Yi X; Liu J; Sun X; Shen S; Yang K; Liu Z, Adv. Mater. 2016, 28, 7143. [PubMed: 27275921]
51. Huang Y; Ren J; Qu X, Chem. Rev. 2019, 119, 4357. [PubMed: 30801188]
52. Wang Z; Zhang Y; Ju E; Liu Z; Cao F; Chen Z; Ren J; Qu X, Nat. Commun. 2018, 9, 3334. [PubMed: 30127408]
53. Yang G; Ji J; Liu Z, WIRES Nanomed. Nanobi. 2021, 13, 1720.
54. Chen Q; Chen J; Yang Z; Xu J; Xu L; Liang C; Han X; Liu Z, Adv. Mater. 2019, 31, 1802228.
55. Horsman M; Mortensen L; Petersen J; Busk M; Overgaard J, Nat. Rev. Clin. Oncol. 2012, 9, 674. [PubMed: 23149893]
56. Pan Y; Tang W; Fan W; Zhang J; Chen X, Chem. Soc. Rev. 2022, 51, 9759. [PubMed: 36354107]
57. Sorensen B; Horsman M, Front. Oncol. 2020, 10, 562. [PubMed: 32373534]
58. Vaupel P, In Seminars in radiation oncology 2004 Jul 1 (Vol. 14, No. 3, pp. 198–206).
59. Jain RK,. Clin. Oncol.2013, 31, 2205.
60. Martin JD; Panagi M; Wang C; Khan TT; Martin MR; Voutouri C; Toh K; Papageorgis P; Mpekris F; Polydorou C, ACS Nano 2019, 13, 6396. [PubMed: 31187975]
61. Huang Y; Yuan J; Righi E; Kamoun WS; Ancukiewicz M; Nezivar J; Santosuosso M; Martin JD; Martin MR; Vianello F, Proc. Natl. Acad. Sci. USA 2012, 109, 17561. [PubMed: 23045683]
62. Hu K; Miao L; Goodwin TJ; Li J; Liu Q; Huang L, ACS Nano 2017, 11, 4916. [PubMed: 28414916]
63. Wang X; Niu X; Sha W; Feng X; Yu L; Zhang Z; Wang W; Yuan Z, Biomater. Sci. 2021, 9, 6308. [PubMed: 34519724]
64. Liu Z; Wang Y; Purro M; Xiong MP, Oxidation-induced degradable nanogels for iron chelation. Sci. Rep. 2016, 6, 1. [PubMed: 28442746]
65. Rees JA; Deblonde GJ-P; An DD; Ansoborlo C; Gauny SS; Abergel RJ, Sci. Rep. 2018, 8, 1. [PubMed: 29311619]
66. Liang C; Chao Y; Yi X; Xu J; Feng L; Zhao Q; Yang K; Liu Z, Biomaterials 2019, 197, 368. [PubMed: 30703742]
67. Fang J; Nakamura H; Maeda H, Adv. Drug Deliv. Rev. 2011, 63, 136. [PubMed: 20441782]
68. Matsumura Y; Maeda H, Cancer Res. 1986, 46, 6387. [PubMed: 2946403]
69. Brach M; Gruss H; Kaisho T; Asano Y; Hirano T; Herrmann F, J. Biol. Chem. 1993, 268, 8466. [PubMed: 8473290]
70. Gajewski TF; Schreiber H; Fu YX, Nat. Immunol. 2013, 14, 10142.
71. Gutiérrez V; Seabra AB; Reguera RM; Khandare J; Calderón M, Chem. Soc. Rev. 2016, 45, 152. [PubMed: 26487097]
72. Vanneman M; Dranoff G, Nat. Rev. Cancer 2012, 12, 2371.
73. Chen Q; Chen M; Liu Z, Chem. Soc. Rev. 2019, 48, 5506. [PubMed: 31589233]
74. Fan W; Tang W; Lau J; Shen Z; Xie J; Shi J; Chen X, Adv. Mater. 2019, 31, 1806381.
75. Hegde AM; Cherry CR; Stroud CRG; Pinnamaneni R; Cherukuri SD; Sharma N; Bowling M; Ju AW; Arastu HH; Walker PR, Am. J. Clin. Oncol. 2018, 36, 21134.
76. Lu YC; Wang XJ, Mol. Carcinog. 2020, 59, 675. [PubMed: 32386070]

77. Cabral H; Miyata K; Osada K; Kataoka K, Chem. Rev. 2018, 118, 6844. [PubMed: 29957926]
78. Irvine DJ; Hanson MC; Rakhra K; Tokatlian T, Chem. Rev. 2015, 115, 11109. [PubMed: 26154342]
79. Wang H; Mooney DJ, Nat. Mater. 2018, 17, 761. [PubMed: 30104668]
80. Ding J; Chen J; Gao L; Jiang Z; Zhang Y; Li M; Xiao Q; Lee SS; Chen X, Nano Today 2019, 29, 100800.
81. Zhou J; Kroll AV; Holay M; Fang RH; Zhang L, Adv. Mater. 2020, 32, 1901255.
82. Wang J; Li Z; Wang Z; Yu Y; Li D; Li B; Ding J, Adv. Funct. Mater. 2020, 30, 1910676.
83. Luo T; Nash G; Jiang X; Feng X; Mao J; Liu J; Juloori A; Pearson A; Lin W, Adv. Mater. 2022, 34, 2110588.
84. Kim J; Mooney DJ, Nano Today 2011, 6, 466. [PubMed: 22125572]
85. Liang C; Xu L; Song G; Liu Z, Chem. Soc. Rev. 2016, 45, 6250. [PubMed: 27333329]
86. Vodnala SK; Eil R; Kishton RJ; Sukumar M; Yamamoto TN; Ha N-H; Lee P-H; Shin M; Patel SJ; Yu Z, Science 2019, 363, eaau0135. [PubMed: 30923193]
87. Wei P; Moodera JS, Nat. Mater. 2020, 19, 481. [PubMed: 32055033]
88. Szebeni J; Simberg D; González-Fernández Á; Barenholz Y; Dobrovolskaia MA, Nat. Nanotechnol. 2018, 13, 1100. [PubMed: 30348955]
89. Cho NH; Cheong TC; Min JH; Wu JH; Lee SJ; Kim D; Yang JS; Kim S; Kim YK; Seong SY, Nat. Nanotechnol. 2011, 6, 675. [PubMed: 21909083]
90. Manaster Y; Shipony Z; Hutzler A; Kolesnikov M; Avivi C; Shalmon B; Barshack I; Besser MJ; Feferman T; Shakhar G, Cancer Immunol. Immunother. 2019, 68, 1287. [PubMed: 31253998]
91. Najjar YG; Menk AV; Sander C; Rao U; Karunamurthy A; Bhatia R; Zhai S; Kirkwood JM; Delgoffe GM, JCI Insight 2019, 4, 124989. [PubMed: 30721155]
92. Zandberg DP; Menk AV; Velez M; Normolle D; DePeaux K; Liu A; Ferris RL; Delgoffe GM, Immunother J. Cancer 2021, 9, 002088.
93. Brooks JM; Menezes AN; Ibrahim M; Archer L; Lal N; Bagnall CJ; Von, Zeidler SV.; Valentine HR; Spruce RJ; Batis N; Bryant JL.; Clin. Cancer Res. 2019, 25, 5315. [PubMed: 31182433]
94. Jaiswal AR; Liu AJ; Pudakalakatti S; Dutta P; Jayaprakash P; Bartkowiak T; Ager CR; Wang ZQ; Reuben A; Cooper ZA; Ivan C, Cancer Immunol. Res. 2020, 8, 1365. [PubMed: 32917656]
95. Facciabene A; Peng X; Hagemann IS; Balint K; Barchetti A; Wang LP; Gimotty PA; Gilks CB; Lal P; Zhang L; Coukos G, Nature 2011, 475, 226. [PubMed: 21753853]
96. Henze AT; Mazzone M, J. Clin. Invest. 2016, 126, 3672. [PubMed: 27482883]
97. Chiu DK; Xu IM; Lai RK; Tse AP; Wei LL; Koh HY; Li LL; Lee D; Lo RC; Wong CM; Ng IO, Hepatol J. 2016, 64, 797.
98. Scharping NE; Rivadeneira DB; Menk AV; Vignali PD; Ford BR; Rittenhouse NL; Peralta R; Wang Y; Wang Y; DePeaux K; Poholek AC, Nat. Immunol. 2021, 22, 205. [PubMed: 33398183]
99. Scharping NE; Menk AV; Whetstone RD; Zeng X; Delgoffe GM, Cancer Immunol. Res. 2017, 5, 9. [PubMed: 27941003]
100. Tian L; Wang Y; Sun L; Xu J; Chao Y; Yang K; Wang S; Liu Z, Matter 2019, 1, 1061.
101. Ni K; Lan G; Chan C; Quigley B; Lu K; Aung T; Guo N; La Riviere P; Weichselbaum RR; Lin W, Nat. Commun. 2018, 9, 2351. [PubMed: 29907739]
102. Liu Y; Dong Y; Kong L; Shi F; Zhu H; Yu J, J. Hematol. Oncol. 2018, 11, 1. [PubMed: 29298689]
103. Hwang W; Pike L; Royce T; Mahal B; Loeffler J, Nat. Rev. Clin. Oncol. 2018, 15, 477. [PubMed: 29872177]
104. Gotwals P; Cameron S; Cipolletta D; Cremasco V; Crystal A; Hewes B; Mueller B; Quaratino S; Sabatos-Peyton C; Petruzzelli L; Engelman JA; Dranoff G, Nat. Rev. Cancer 2017, 17, 286. [PubMed: 28338065]
105. Topalian SL; Taube JM; Anders RA; Pardoll DM, Nat. Rev. Cancer 2016, 16, 275. [PubMed: 27079802]
106. Sanmamed MF; Chen L, Cell 2018, 175 313. [PubMed: 30290139]
107. Sun L; Shen F; Tian L; Tao H; Xiong Z; Xu J; Liu Z, Adv. Mater. 2021, 33, 2007910.

108. Conniot J; Scomparin A; Peres C; Yeini E; Pozzi S; Matos AI; Kleiner R; Moura LIF; Zupancic E; Viana AS; Doron H; Gois PMP; Erez N; Jung S; Satchi-Fainaro R; Florindo HF, Nat. Nanotechnol. 2019, 14, 891. [PubMed: 31384037]
109. Chen Q; Wang C; Zhang X; Chen G; Hu Q; Li H; Wang J; Wen D; Zhang Y; Lu Y, Nat. Nanotechnol. 2019, 14, 89. [PubMed: 30531990]
110. Derer A; Frey B; Fietkau R; Gaipl U, Cancer Immunol. Immunother. 2016, 65, 779. [PubMed: 26590829]
111. Victor T; Rech A; Maity A; Rengan R; Pauken K; Stelekati E; Benci J; Xu B; Dada H; Odorizzi P; Herati R, Nature 2015, 520, 373. [PubMed: 25754329]
112. Vander Heiden MG; DeBerardinis RJ, Cell 2017, 168, 657. [PubMed: 28187287]
113. Gao F; Tang Y; Liu WL; Zou MZ; Huang C; Liu CJ; Zhang XZ, Adv. Mater. 2019, 31, 1904639.
114. Gatenby RA; Gillies RJ, Nat. Rev. Cancer 2004, 4, 891. [PubMed: 15516961]
115. Zhai L; Spranger S; Binder DC; Gritsina G; Lauing KL; Giles FJ; Wainwright DA, Clin. Cancer Res. 2015, 21, 5427. [PubMed: 26519060]
116. Park HJ; Lee SH; Chung H; Rhee YH; Lim BU; Ha SW; Griffin RJ; Lee HS; Song CW; Choi EK, Radiat. Res. 2003, 159, 86. [PubMed: 12492371]
117. Park H; Lyons JC; Griffin RJ; Lim BU; Song CW, Radiat. Res. 2000, 153, 295104.
118. Czystowska Kuzmicz M; Sosnowska A; Nowis D; Ramji K; Szajnik M; Chlebowska-Tuz J; Wolinska E; Gaj P; Grazul M; Pilch Z, Nat. Commun. 2019, 10, 1. [PubMed: 30602773]
119. Zhang H; Liu J; Qu D; Wang L; Wong CM; Lau C-W; Huang Y; Wang YF; Huang H; Xia Y, Proc. Natl. Acad. Sci. USA 2018, 115, 6927.
120. Yu M; Guo G; Huang L; Deng L; Chang CS; Achyut BR; Canning M; Xu N; Arbab AS; Bollag RJ, Nat. Commun. 2020, 11, 1. [PubMed: 31911652]
121. Gao J; Wang Z; Guo Q; Tang H; Wang Z; Yang C; Fan H; Zhang W; Ren C; Liu J, Theranostics 2022, 12, 1286. [PubMed: 35154487]
122. Guo Y; Xie YQ; Gao M; Zhao Y; Franco F; Wenes M; Siddiqui I; Bevilacqua A; Wang H; Yang H, Nat. Immunol. 2021, 22, 746. [PubMed: 34031618]
123. Xue CC; Li MH; Sutrisno L; Yan BB; Zhao Y; Hu Y; Cai KY; Zhao Y; Yu SH; Luo Z, Adv. Funct. Mater. 2021, 31, 2008732.
124. Dong Z; Feng L; Hao Y; Li Q; Chen M; Yang Z; Zhao H; Liu Z, Chem 2020, 6, 1391.
125. Xue CC; Li MH; Zhao Y; Zhou J; Hu Y; Cai KY; Zhao Y; Yu SH; Luo Z, Sci. Adv. 2020, 6, 1346.
126. Wang C; Dong Z; Hao Y; Zhu Y; Ni J; Li Q; Liu B; Han Y; Yang Z; Wan J, Adv. Mater. 2022, 34, 2106520.
127. Ni K; Aung T; Li S; Fatuzzo N; Liang X; Lin W, Chem 2019, 5, 1892. [PubMed: 31384694]
128. Dong Z; Wang C; Gong Y; Zhang Y; Fan Q; Hao Y; Li Q; Wu Y; Zhong X; Yang K; Feng L, ACS Nano 2022, 16, 13884. [PubMed: 36075132]
129. Shen H; Hau E; Joshi S; Dilda P; McDonald K, Mol. Cancer. Ther. 2015, 14, 1794. [PubMed: 26063767]
130. Kolb D; Kolishetti N; Surnar B; Sarkar S; Dhar S, ACS Nano 2020, 9, 11055.
131. Boroughs L; DeBerardinis R, Nat. Cell Biol. 2015, 17, 351. [PubMed: 25774832]
132. Jiang W; Luo X; Wei L; Yuan S; Cai J; Jiang X; Hu Y, Small 2021, 17, 2102695.
133. Liu X; Li Y; Wang K; Chen Y; Shi M; Zhang X; Pan W; Li N; Tang B, Nano Lett. 2021, 21, 7862. [PubMed: 34494442]
134. Li K; Lin C; He Y; Lu L; Cai K, ACS Nano 2020, 14, 14164. [PubMed: 32975406]
135. Park CC; Henshall-Powell RL; Erickson AC; Talhouk R; Parvin B; Bissell MJ; Barcellos-Hoff MH, Proc. Natl. Acad. Sci. USA 2003, 100, 10728. [PubMed: 12960393]
136. Ji TJ; Zhao Y; Ding YP; Nie GJ, Adv. Mater. 2013, 25, 3508. [PubMed: 23703805]
137. Cheng Y; Zhu J; Zhao L; Xiong Z; Tang Y; Liu C; Guo L; Qiao W; Shi X; Zhao J, Nanomedicine. 2016, 11, 1253. [PubMed: 26940668]
138. Wu J; Chen J; Feng Y; Zhang S; Lin L; Guo Z; Sun P; Xu C; Tian H; Chen X, Sci. Adv. 2020, 6, 7828.
139. Kalluri R, Nat. Rev. Cancer 2016, 16, 582. [PubMed: 27550820]

140. Chen X; Song E, Nat. Rev. Drug Discov. 2019, 18, 99. [PubMed: 30470818]
141. Costa A; Kieffer Y; Scholer-Dahirel A; Pelon F; Bourachot B; Cardon M; Sirven P; Magagna I; Fuhrmann L; Bernard C, Cancer cell 2018, 33, 463. [PubMed: 29455927]
142. Ni K; Xu Z; Culbert A; Luo T; Guo N; Yang K; Pearson E; Preusser B; Wu T; Riviere PL; Weichselbaum RR; Spiotto MT; Lin W, Nat. Biomed. Eng. 2022, 6, 144. [PubMed: 35190678]
143. Zong Z; Zhang Z; Wu L; Zhang L; Zhou F, Adv. Sci. 2021, 8, 2002484.
144. Corrales L; McWhirter SM; Dubensky TW Jr; Gajewski TF., J. Clin. Invest. 2016, 126 2404. [PubMed: 27367184]
145. Su T; Zhang Y; Valerie K; Wang X; Lin S; Zhu G, Theranostics 2019, 9, 7759. [PubMed: 31695799]
146. Junkins R; Gallovic M; Johnson B; Collier M; Watkins-Schulz R; Cheng N; David C; McGee C; Sempowski G; Shterev I; McKinnon K, Contr J. Release 2018, 270, 1.
147. Yan J; Wang G; Xie L; Tian H; Li J; Li B; Sang W; Li W; Zhang Z; Dai Y, Adv. Mater. 2022, 34, 2105783.
148. Yang K; Han W; Jiang X; Piffko A; Bugno J; Han C; Li S; Liang H; Xu Z; Zheng W; Wang L, Nat. Nanotechnol. 2022, DOI: 10.1038/s41565-022-01225-x.
149. Zhu Y; An X; Zhang X; Qiao Y; Zheng T; Li X, Mol. Cancer 2019, 18, 152. [PubMed: 31679519]
150. Chin E; Yu C; Vartabedian V; Jia Y; Kumar M; Gamo A; Vernier W; Ali S; Kissai M; Lazar D; Nguyen N, Science 2020, 369, 993 [PubMed: 32820126]
151. Ren Z; Sun S; Sun R; Cui G; Hong L; Rao B; Li A; Yu Z; Kan Q; Mao Z, Adv. Mater. 2020, 32, 1906024.
152. Zheng H; Guo B; Qiu X; Xia Y; Qu Y; Cheng L; Meng F; Zhong Z, Bioact. Maters. 2022, 16, 1.

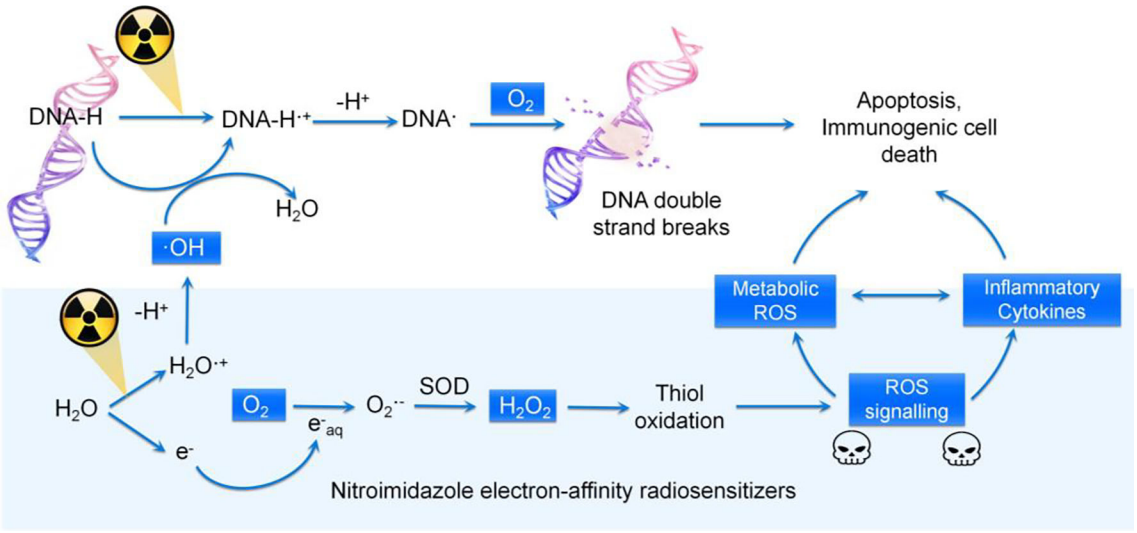

Figure 1.
Proposed mechanisms of radiosensitization by O_2.[42]

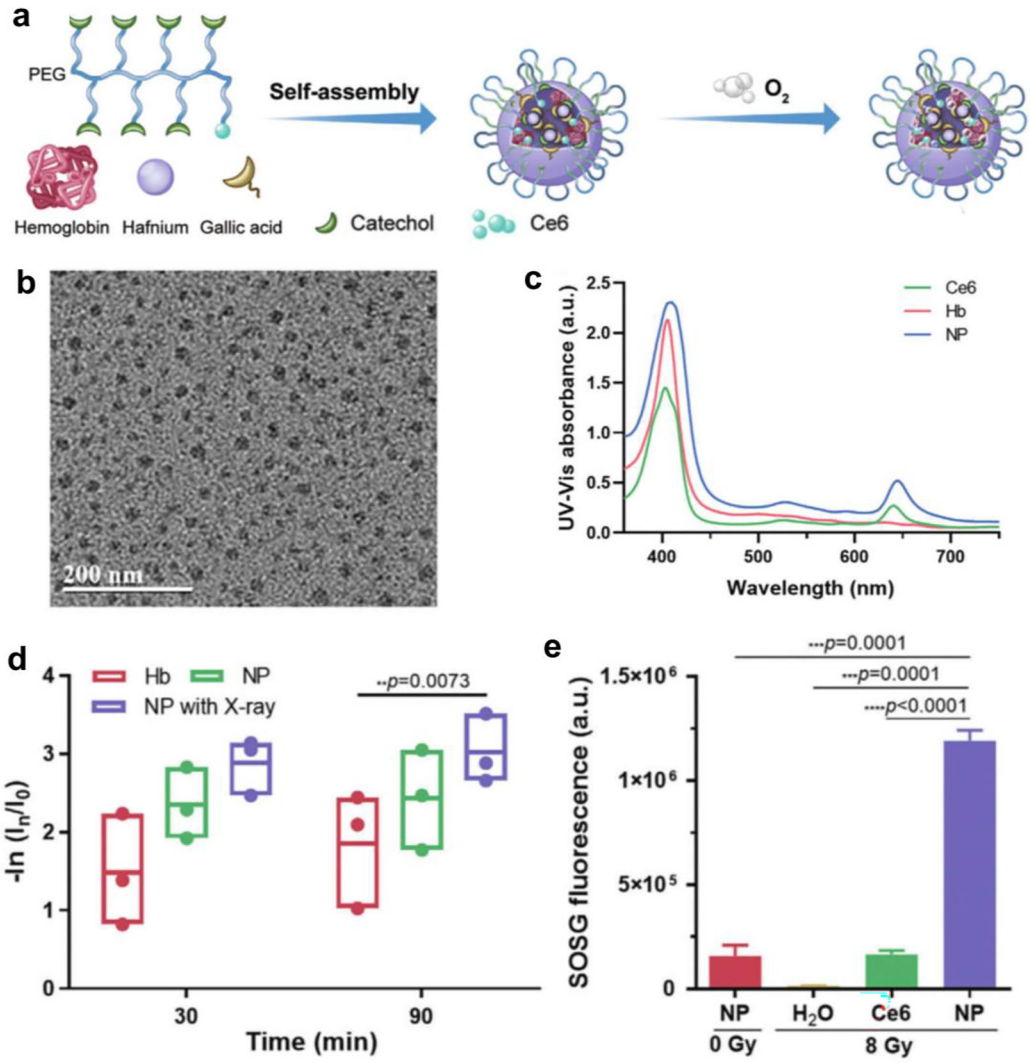

Figure 2.

(a) Schematic showing the synthesis of Hb@Hf-Ce6. (b) TEM image of Hb@Hf-Ce6 NPs. (c) UV-vis absorption spectra of chlorin e6 (Ce6), hemoglobin (Hb), and Hb@Hf-Ce6. (d) Oxygen release behaviors of Hb and Hb@Hf-Ce6 with and without X-ray irradiation. (e) Generation of $^1O_2$ as detected by singlet oxygen sensor green (SOSG).[48] Copyright 2020, John Wiley and Sons.

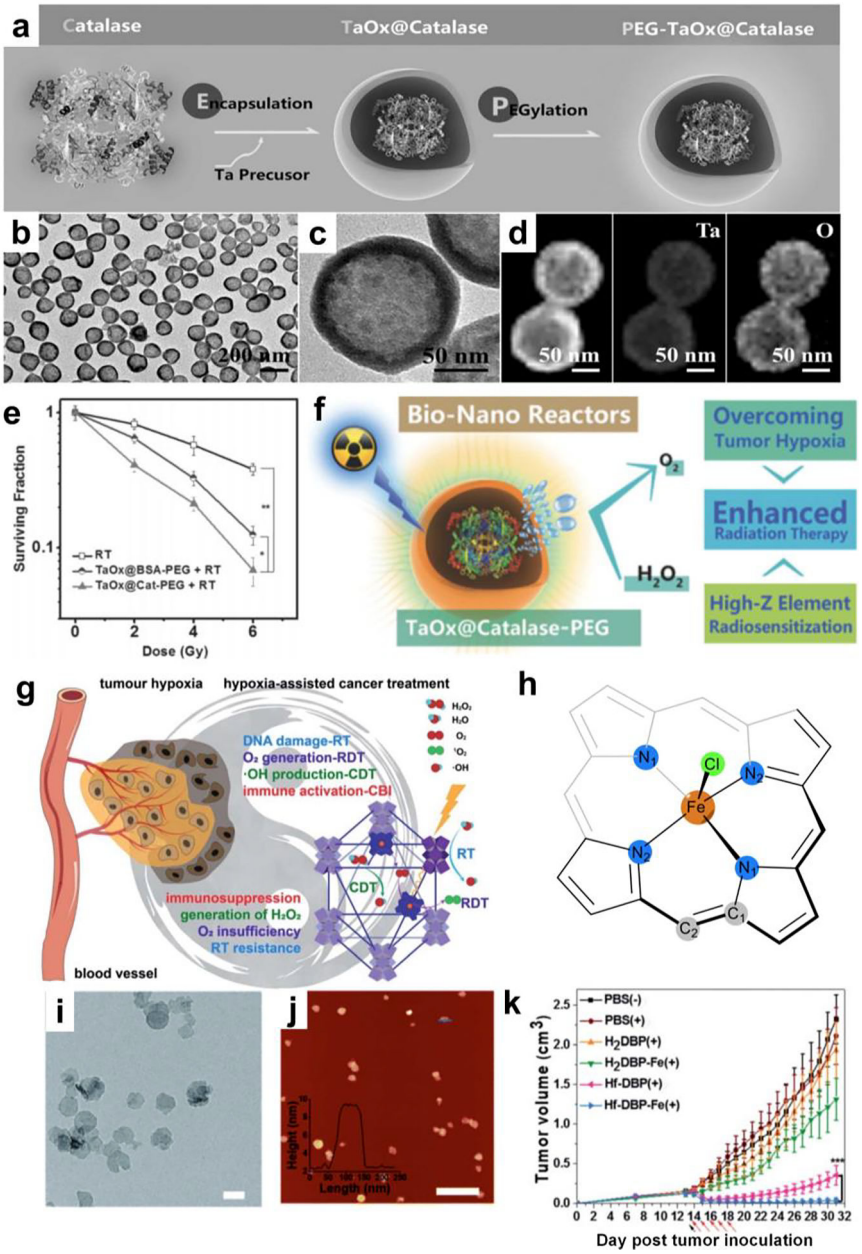

Figure 3.

(a) Synthesis of TaO_x@Catalase hollow nanospheres. (b) TEM image and (c) magnified TEM image of TaO_x@Catalase. (d) HAADF-STEM image and elemental mapping. (e) Clonogenic assay of 4T1 cells incubated with PEG-TaO_x@BSA and PEG-TaO_x@Catalase. (f) Schematic illustration of the decomposition of H_2O_2 to O_2 by PEG-TaO_x@Catalase for synergistic enhancement of the overall therapeutic efficacy.[50] Copyright 2016, John Wiley and Sons. (g) Hf-DBP-Fe nMOFs relieved tumor hypoxia to enhance the overall therapeutic effect. (h) Molecular model of porphyrin-Fe-Cl for EXAFS fitting. TEM image (i) and AFM topography and its height profile (inset) along the blue line of Hf-DBP-Fe (j). (k) Growth curves of MC38 tumors with different treatments. Black arrows and red arrows indicate

the injection of therapeutic agents and X-ray irradiation, respectively.[6] Copyright 2020, the Royal Society of Chemistry.

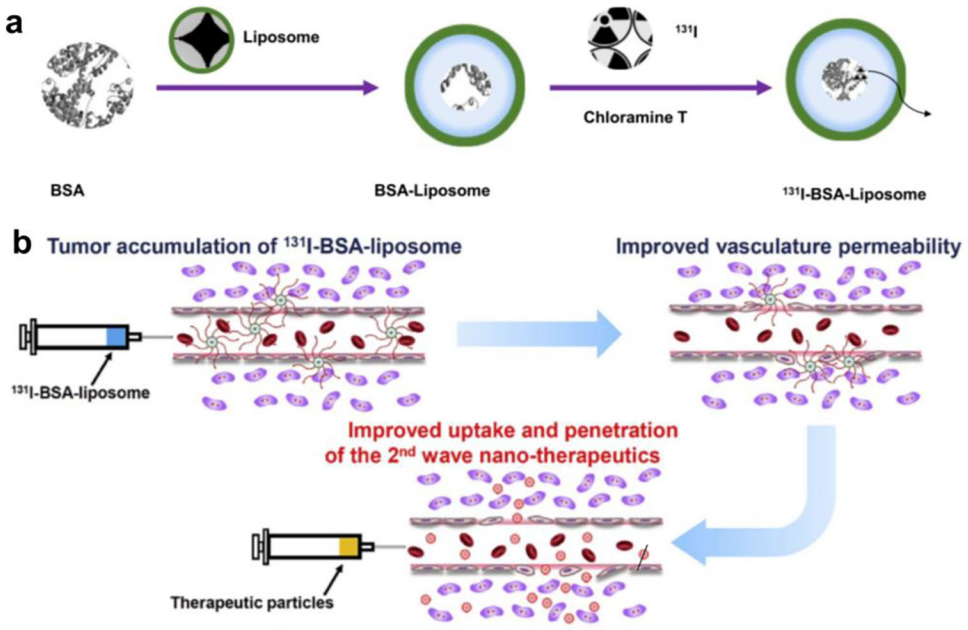

Figure 4.

(a) Schematic illustrating the preparation of ^{131}I-BSA-liposome. (b-d) Proposed mechanism for improving tumor vascular permeability: (b) ^{131}I-BSA-liposome accumulates around blood vessels after i.v. injection, β-rays from ^{131}I destroy blood vasculature endothelial cells to increase the permeability of blood vessels, and second-wave nanotherapeutics penetrate and accumulate in tumors.[66] Copyright Elsevier, 2019.

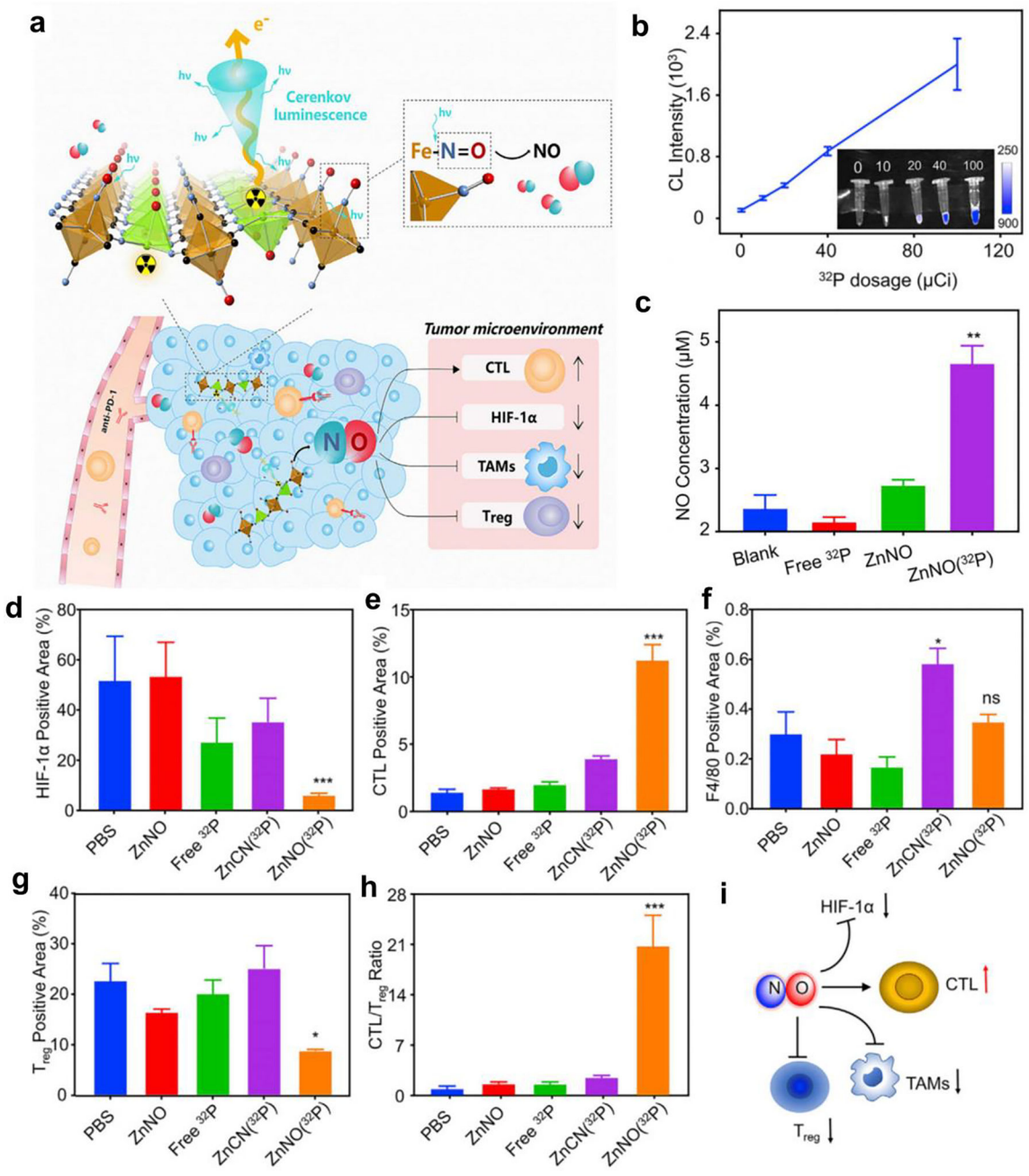

Figure 5.

(a) Schematic illustration of remodeling hypoxic and immunosuppressive TMEs to enhance the therapeutic effect of $ZnFe(CN)_5NO(P^{32})$ nanosheets via continuous release of NO triggered by radioisotope-induced Cerenkov luminescence. (b) CL intensity at different ^{32}P doses. Inset: CL images of ^{32}P. (c) Concentration of NO in the supernatant of cell culture medium. HIF-α-positive (d), CTL-positive (e), F4/80-positive (f), and Treg-positive (g) areas in tumors after different treatments. (h) CTL/Treg ratios after different treatments. (i) Regulation of TME by the release of NO stimulated by CL.[100] Copyright 2019, Elsevier.

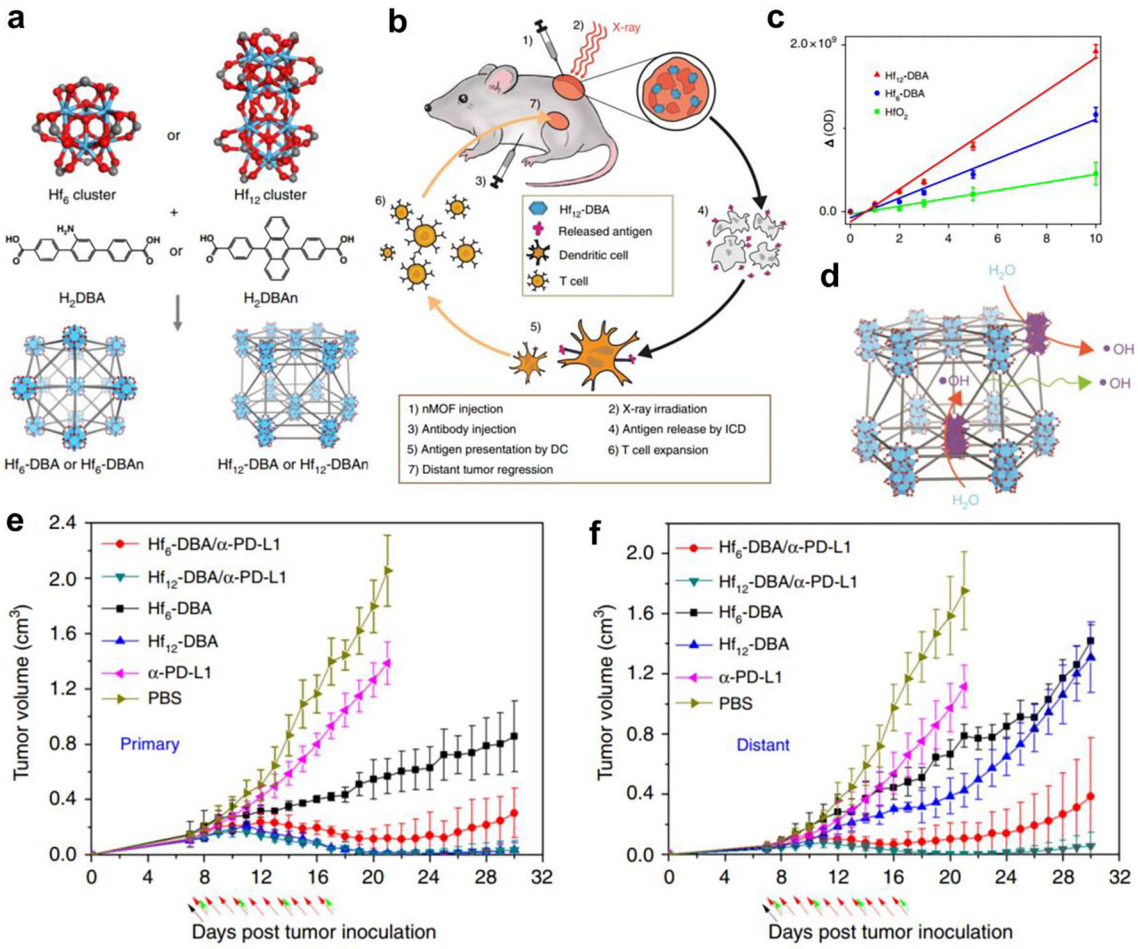

Figure 6.

(a) Preparation of Hf_6-DBA and Hf_{12}-DBA. (b) A bilateral tumor model was used to study the abscopal effect of nMOF-mediated RT in combination with anti-PD-L1 to enhance the expansion and infiltration of effective T cells for distant tumor control. (c) Aminophenyl fluorescein fluorescence after irradiating HfO_2, Hf_6-DBA, and Hf_{12}-DBA aqueous solutions. (d) Generation of •OH upon X-ray irradiation and diffusion through porous Hf_{12}-DBA nanoplates. Growth curves of primary (e) and distant CT26 tumors (f) with different treatments.[101] Copyright 2018, Springer Nature.

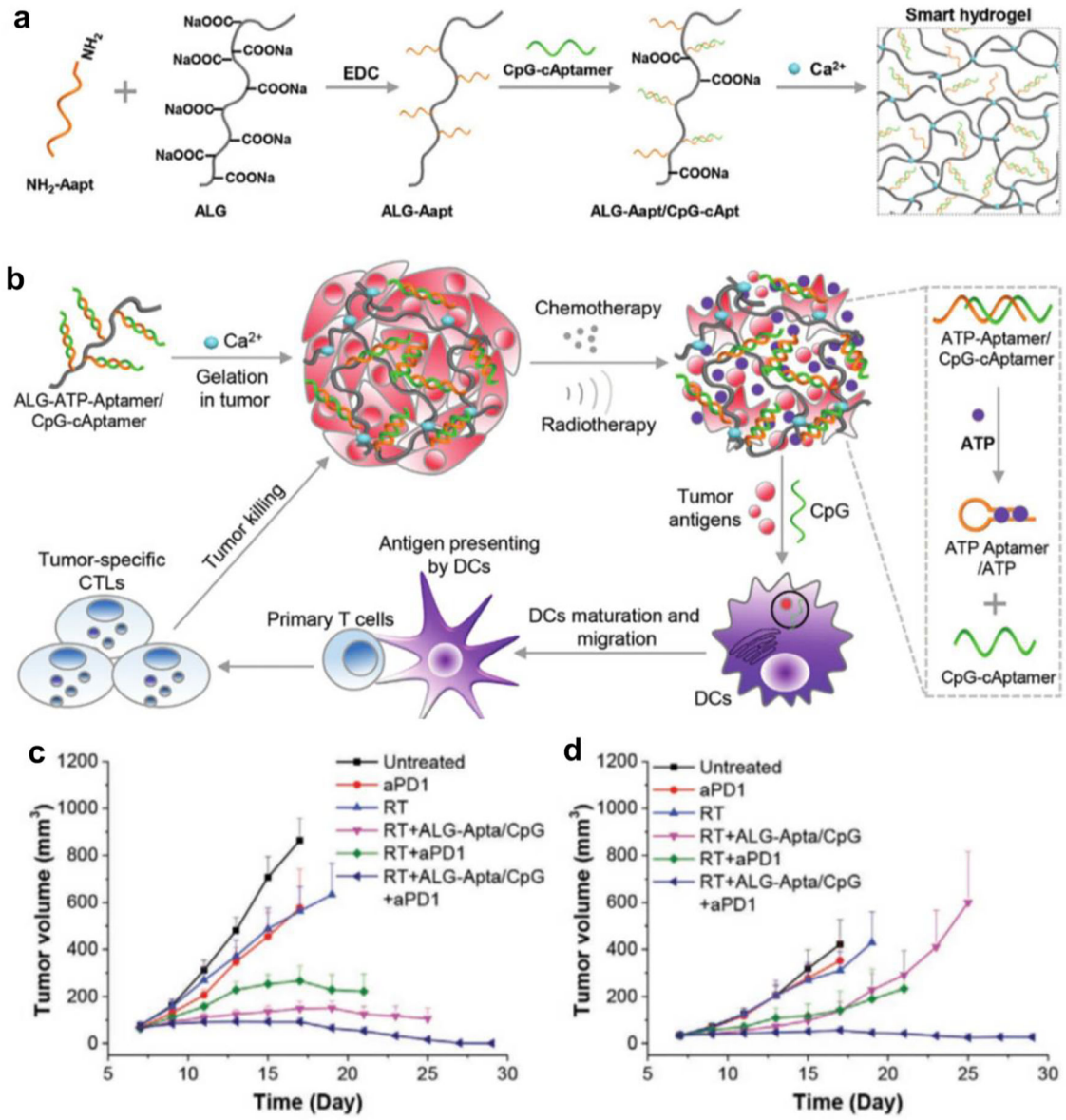

Figure 7.

(a) Preparation of a hydrogel composed of ALG, ATP-specific aptamer (Aapt), and CpG-cAptamer (CpG-cApt). (b) Schematic showing triggered release of immune adjuvant in response to ATP released from cancer cells during chemotherapy or RT. Growth curves of primary (c) and distant CT26 tumors (d) with different treatments.[107] Copyright 2021, John Wiley and Sons.

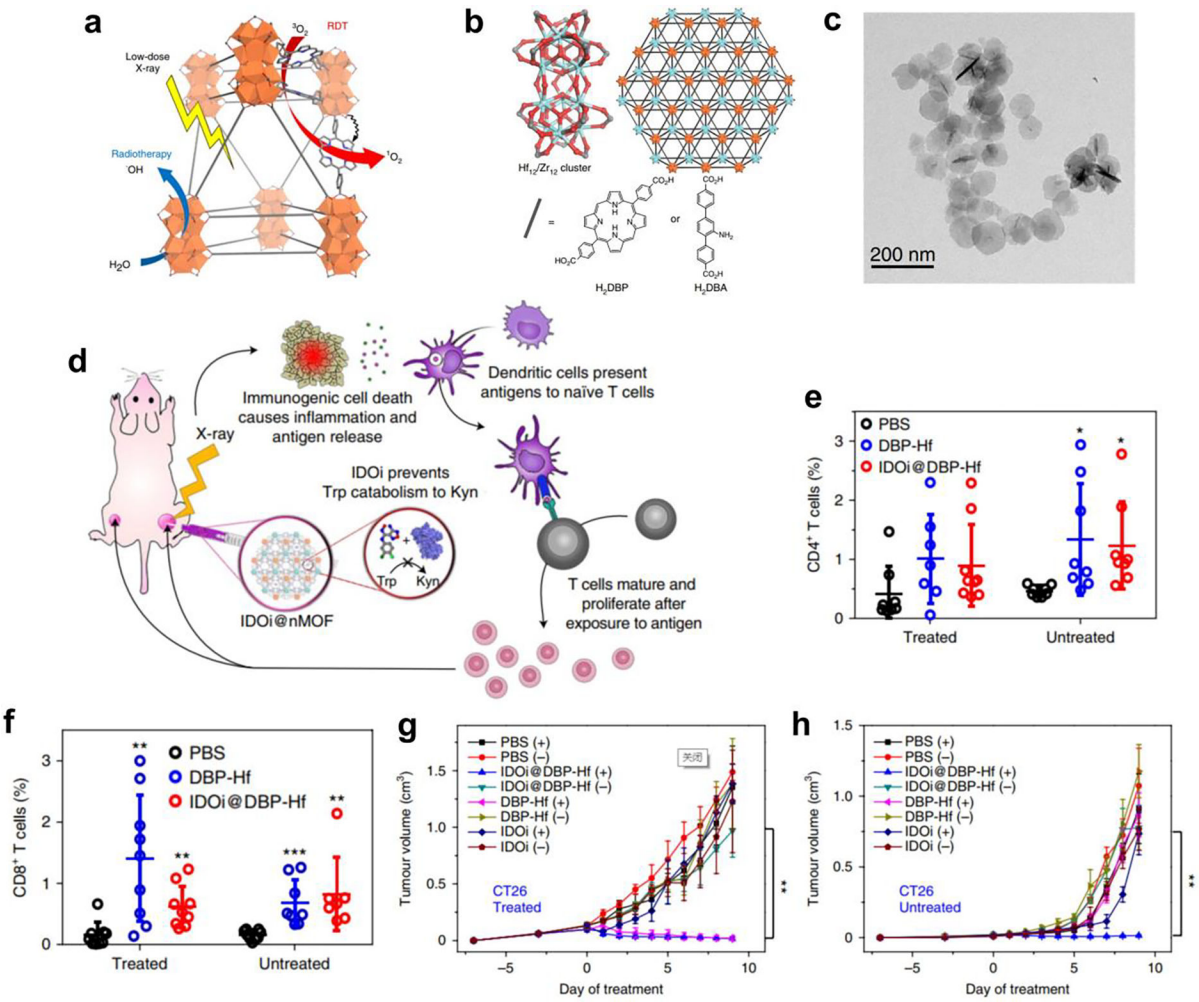

Figure 8.

(a) X-ray induced RT and RDT by nMOFs. (b) Structure models of Hf_{12} secondary building units (SBUs), and DBP-Hf and DBA-Hf nMOFs. (c) TEM image of DBP-Hf. (d) The synergy between RT-RDT and immunotherapy by IDOi@nMOFs led to systemic antitumor immunity. $CD4^+$ T cells (e) and $CD8^+$ T cells (f) in the treated and untreated tumors analyzed by flow cytometry. Growth curves of primary (g) and distant (h) CT26 tumors with different treatments.[49] Copyright 2018, Springer Nature.

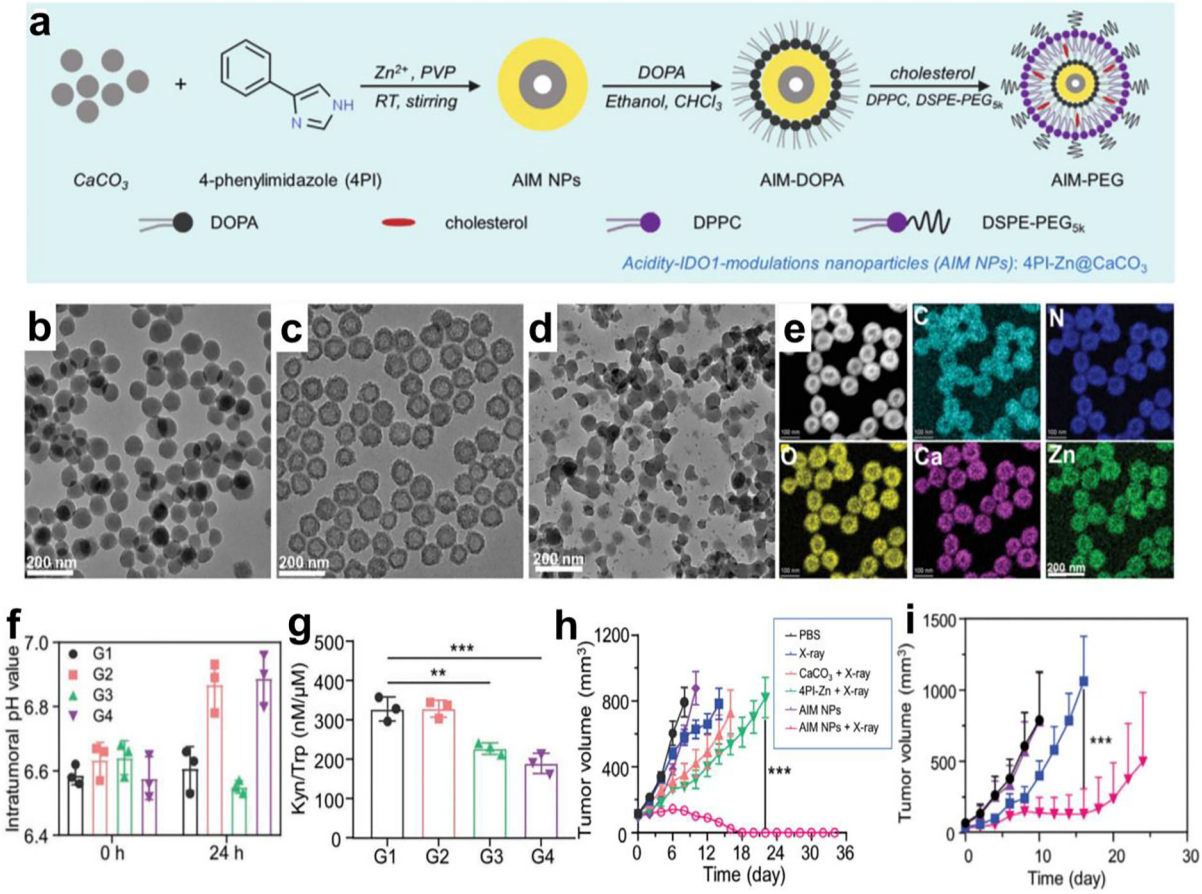

Figure 9.

(a) Preparation of NPs ($CaCO_3$, 4PI-Zn, or AIM NPs). TEM images of (b) $CaCO_3$ NPs, (c) AIM NPs, and (d) 4PI-Zn NPs. (e) STEM image of AIM NPs. (f) Variation of pH values inside tumors before (0 h) and post various injections (24 h) as indicated. G1: PBS; G2: $CaCO_3$; G3: 4PI-Zn; G4: AIM NPs. (g) The Kyn/Trp ratios of the tumors on the mice after i. v. injections of different solutions at 24 h. (h) CT26 tumor growth curves with different treatments. (i) Distant CT26 tumor growth curves with different treatments.[126] Copyright 2020, John Wiley and Sons.

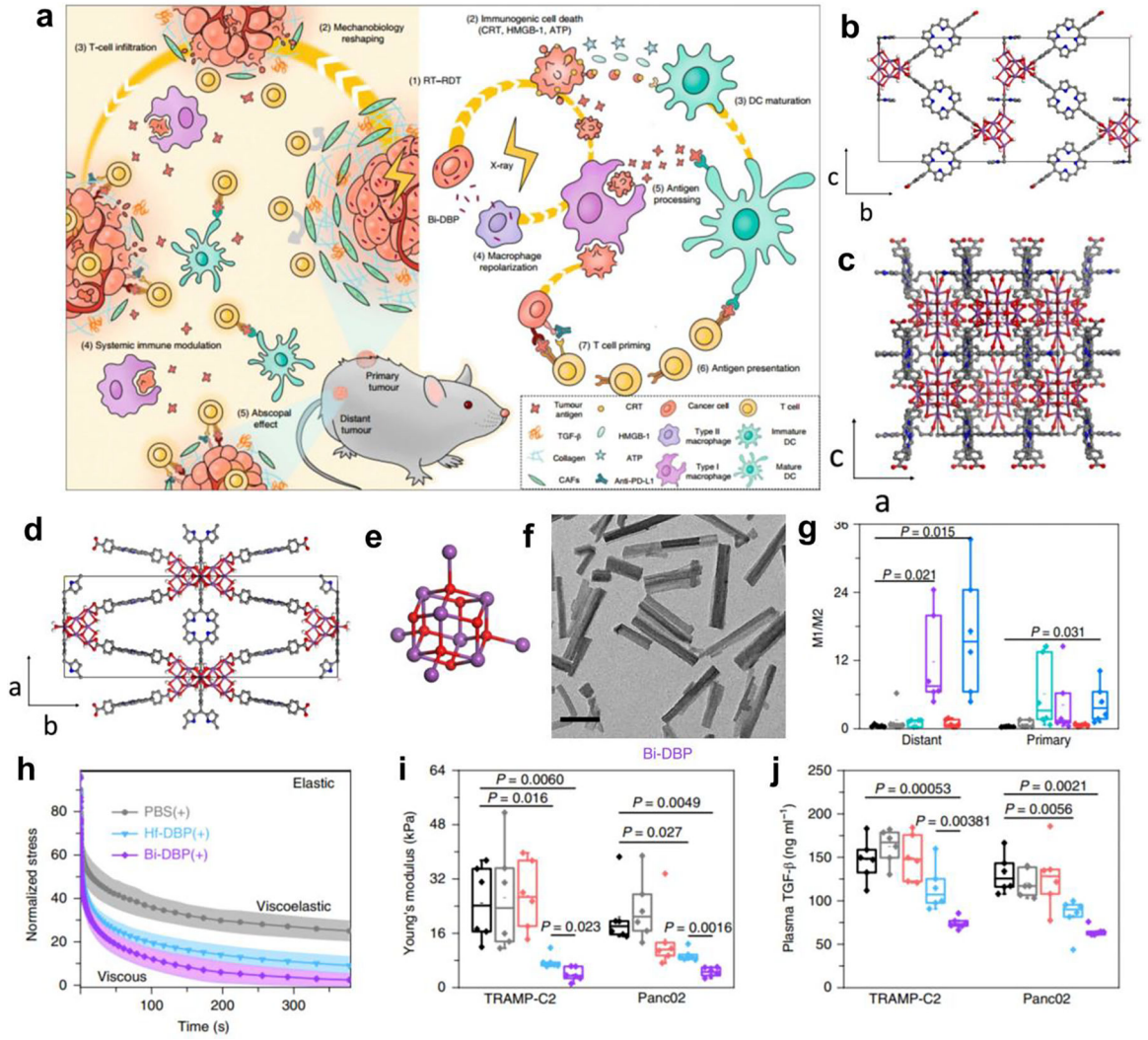

Figure 10.

(a) Schematic illustration of Bi-DBP-mediated RT-RDT for modulating the biomechanic property of tumor tissue and enhancing the immune response. Structure models of Bi-DBP projected along the a-axis (b), the b-axis (c), and the c-axis (d) and $Bi_{10}O_8$ SBU (e). Purple: bismuth; red: oxygen; blue: nitrogen; grey: carbon. (f) TEM image of Bi-DBP. Scale bar: 100 nm. (g) Variation of the M1/M2 ratio in the primary and distant TRAMP-C2 tumors. (h) Stress relaxation of TRAMP-C2 tumors after being intratumorally injected with different solutions upon X-ray irradiation. (i) Young's modulus of TRAMP-C2 or Panc02 tumors after treatment. (j) The concentration of TGF-β in the plasma of TRAMP-C2 or Panc02 tumor-bearing mice after treatment.[142] Copyright 2022, Springer Nature.

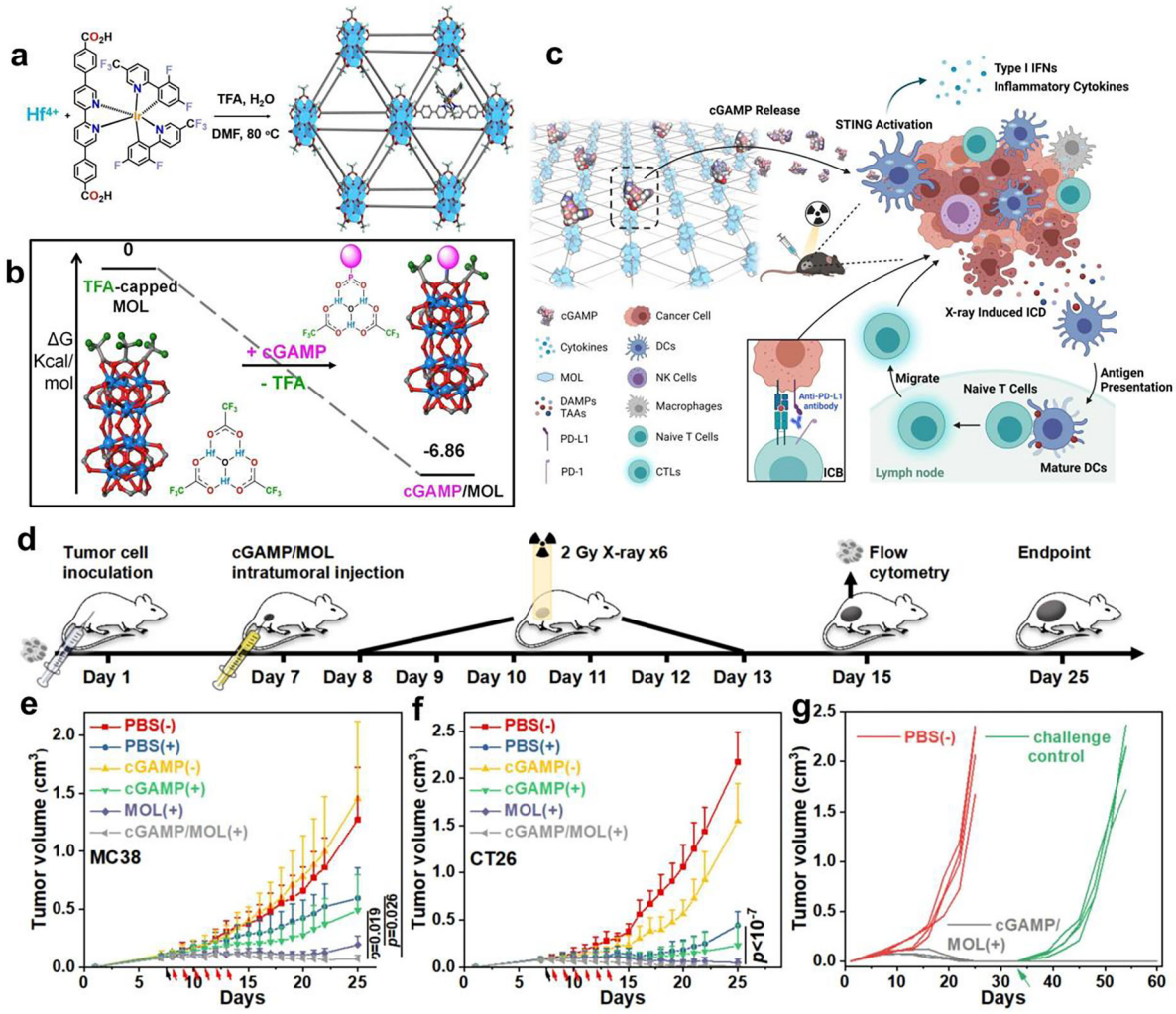

Figure 11.

(a) Preparation of Hf_{12}-Ir MOL. (b) Free energy profiles of TFA substitution by cGAMP. (c) Schematic showing radiosensitization and stimulation of immune responses by cGAMP/MOL. (d) Treatment schema. Growth curves of MC38 (e) and CT26 (f) tumors. The black and red arrows represent intratumoral injection and X-ray irradiation, respectively. (g) Tumor growth curves after tumor challenge and re-challenge of cured BALB/c mice.[83] Copyright 2022, John Wiley and Sons.

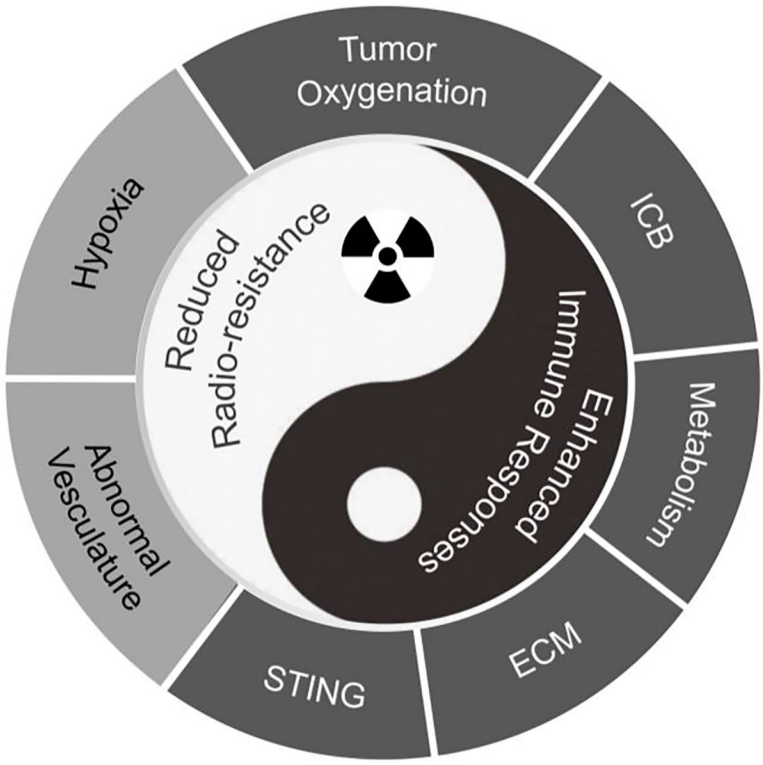

Scheme 1.

Schematic illustration of RT-mediated TME remodeling to reduce radio-resistance and enhance antitumor immune responses.

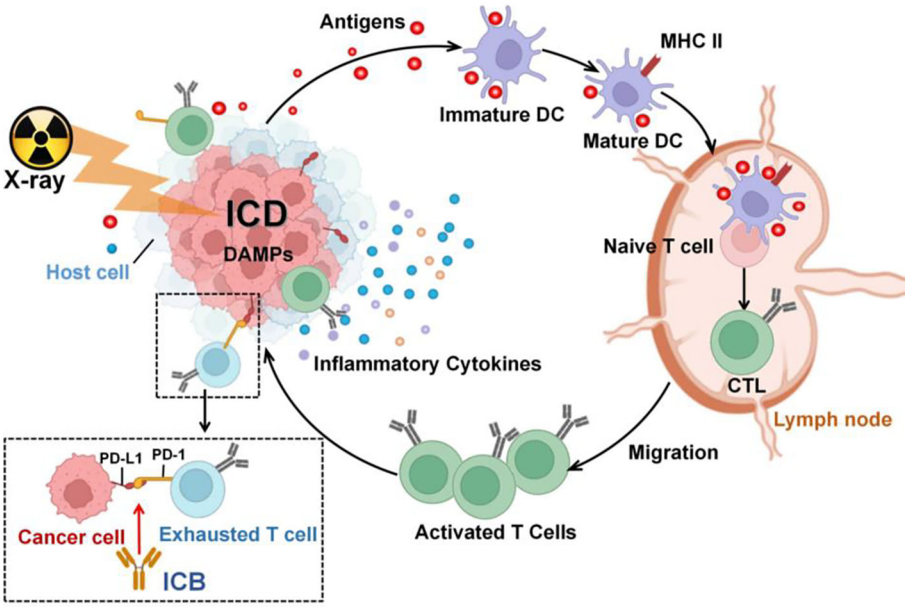

Scheme 2.

Potential mechanisms of anti-tumor immune responses after RT. ICD of cancer cells induced by RT triggers the release of tumor and self antigens and damage-associated molecular patterns (DAMPs) that activate APCs. The activated APCs migrate to draining lymph nodes to prime and activate naive T cells. RT increases T cell receptor (TCR) repertoire of circulating T cells and releases inflammatory chemokines and cytokines that recruit immune cells to the TME, leading to antitumor immune responses.